CR-184115

T. A. Parnell
ES62

LDEF Experiment P0006
LINEAR ENERGY TRANSFER SPECTRUM MEASUREMENT
(LETSME) Quick Look Report

Final Report
Contract No. NAS8-38188
George C. Marshall Space Flight Center
National Aeronautics and Space Administration
Mashall Space Flight Center, AL 35812

19 December 1990

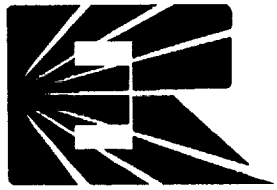

Eril Research, Inc.
P. O. Box 265
Corte Madera, CA 94925

N91-19223

(NASA-CR-184115) LDEF EXPERIMENT P0006 LINEAR ENERGY TRANSFER SPECTRUM MEASUREMENT (LETSME) QUICK LOOK REPORT Final Report (Eril Research) 49 p

CSCL 07A G3/23

Unclas 0333463

LDEF Experiment P0006
LINEAR ENERGY TRANSFER SPECTRUM MEASUREMENT
(LETSME) Quick Look Report

Abstract: The P0006 Quick Look report consists of a preliminary analysis of the various passive radiation detector materials included in the P0006 LETSME experiment flown on LDEF. This work consists of four tasks: 1) readout and analysis of TLDs; 2) readout and analysis of fission foil/mica detectors; 3) readout and analysis of ^{6}LiF/CR-39 detectors; and 4) preliminary processing and readout of CR-39 and polycarbonate PNTDs. TLDs yielded dose rates ranging from 126 $\pm$ 6 mrad/d under 13.4 g/cm^2 total shielding thickness to 307 $\pm$ 11 mrad/d under 1.1 g/cm^2 total shielding thickness. High energy (> 1 MeV) proton dose rate measured from fission foil/mica detectors was 93 mrad/d. High energy neutron dose equivalent rate measured from fission foil/mica detectors was 22 mrem/d. Thermal and resonance neutrons dose equivalent rates measured from ^{6}LiF/CR-39 detectors were 5.9 $\pm$ 1.1 $\times$ 10^{-3} mrem/d ($E_n \leq 0.2$ eV) and 0.33 $\pm$ 0.16 mrem/d (0.2 eV < E_n < 1 MeV). Single surface track fluences on polycarbonate PNTDs ranged from 3.2 $\pm$ 0.07 $\times$ 10^3 to 7.0 $\pm$ 0.16 $\times$ 10^3 tracks/cm^2 for Sheffield PNTD and 3.1 $\pm$ 0.07 $\times$ 10^3 to 10.3 $\pm$ 0.23 $\times$ 10^3 tracks/cm^2 from Tuffak PNTD. Total fluence of particles on CR-39 was 2.127 $\times$ 10^4 tracks/cm^2 for CR-39 and 2.217 $\times$ 10^4 tracks/cm^2 for CR-39 with DOP.

Introduction

The LDEF mission provided a unique and unprecedented opportunity to gather data on the space radiation environment in low earth orbit. This information will be invaluable in addressing the numerous issues concerning the ionizing radiation environment in space and its impact on manned and unmanned space missions. The P0006 experiment, "Linear Energy Transfer Spectrum Measurement" (LETSME), included aboard LDEF, monitored the Linear Energy Transfer (LET) spectra of HZE (High atomic number Z and Energy) particles. In addition, the P0006 experiment measured the total absorbed dose of ionizing radiation, the flux of high energy neutrons and protons and the dose from thermal and resonance neutrons.

The radiation dose (rad) and dose equivalent (rem) will be determined from the P0006 radiation sensitive detectors. This information will be used in predicting the dose and dose equivalent to humans and biological targets in future space flight. Special attention will be paid to measurements of the highly ionizing (high LET) component in assessing the

effectiveness of quality factors (QF) in calculating dose equivalent. Several computer models have been developed to predict the trapped proton and electrons fluxes and the flux of cosmic rays in earth orbit. Measurements from the P0006 experiment will be used to confirm the accuracy of these models and to extend the usefulness of these models to include the East-West trapped proton anisotropy and variations in the space radiation environment due to the 11 year solar cycle. Data from the P0006 experiment will also be used in determining the importance of secondary particles to overall dose and dose equivalent measurements.

Several types of Plastic Nuclear Track Detector (PNTD) made up the bulk of the P0006 experiment. CR-39 PNTD is sensitive to ionizing radiation of $LET_{\infty}\cdot H_2O \geq 5$ keV/μm. Tuffak and Sheffield polycarbonate PNTD are sensitive to ionizing particles with $LET_{\infty}\cdot H_2O \geq 250$ keV/μm while Melinex polyester PNTD is sensitive to radiation of $LET_{\infty}\cdot H_2O \geq 300$ keV/μm. The PNTDs will be used to calculate the LET flux, dose rate and dose equivalent rate spectra. Preliminary LET spectra from the CR-39 detectors is included in this report. In addition, two types of thermoluminescent detectors (TLDs) were used to record total absorbed dose. Fission foil/mica detectors were used to measure high energy neutrons and protons. ^{6}LiF/CR-39 detectors were used for thermal and resonance neutron measurements.

The flight experiment was enclosed in a single flanged canister with an O-ring seal to contain the internal air. The dimensions of the canister are given in Figure 1, the enclosed detector stack and its major components are shown in Figure 2 and the distribution of flight materials in the stack is given in detail in Table 1. In order to compensate for directional dependence of the PNTDs, the detectors were oriented in an orthogonal relationship, with a large stack perpendicular to the z-axis and smaller side stacks oriented perpendicular to the x and y axes.

The LDEF spacecraft was gravity gradient stabilized so that it orbited the earth in a fixed orientation. The P0006 experiment was contained in tray F2, close to the trailing edge of the spacecraft (see Figure 3). Other experiments containing similar radiation detectors were located at different positions on the LDEF. Comparison of results from these different detectors will show the effect of the East-West trapped proton anisotropy. In addition, the shielding of the various radiation measurement experiments is known and will be used to assess the effectiveness of shielding different components of the ionizing radiation environment.

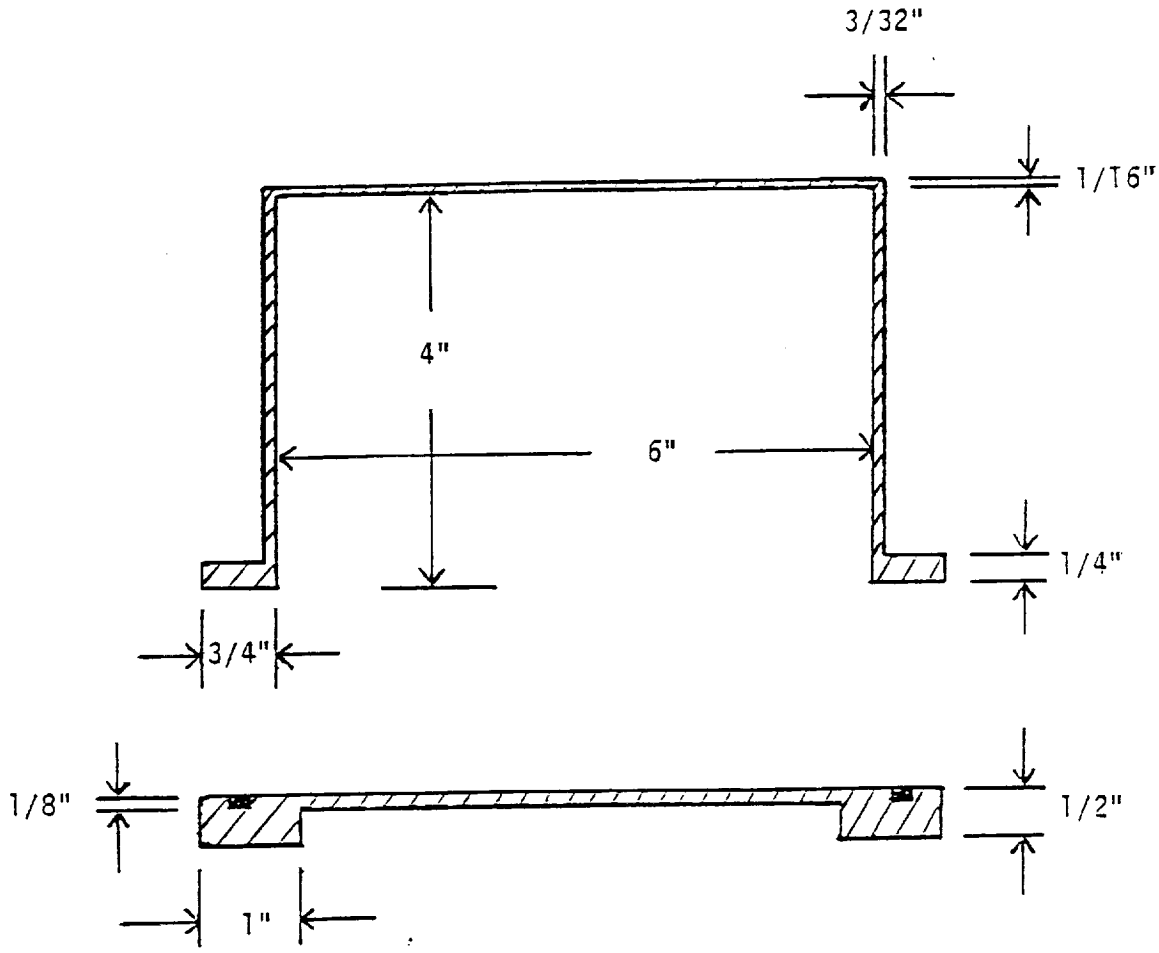

Figure 1: Sketch of the canister for the P0006 experiment.

Configuration of Linear Energy Transfer (LET) Spectrum Measurement Experiment (P0006).

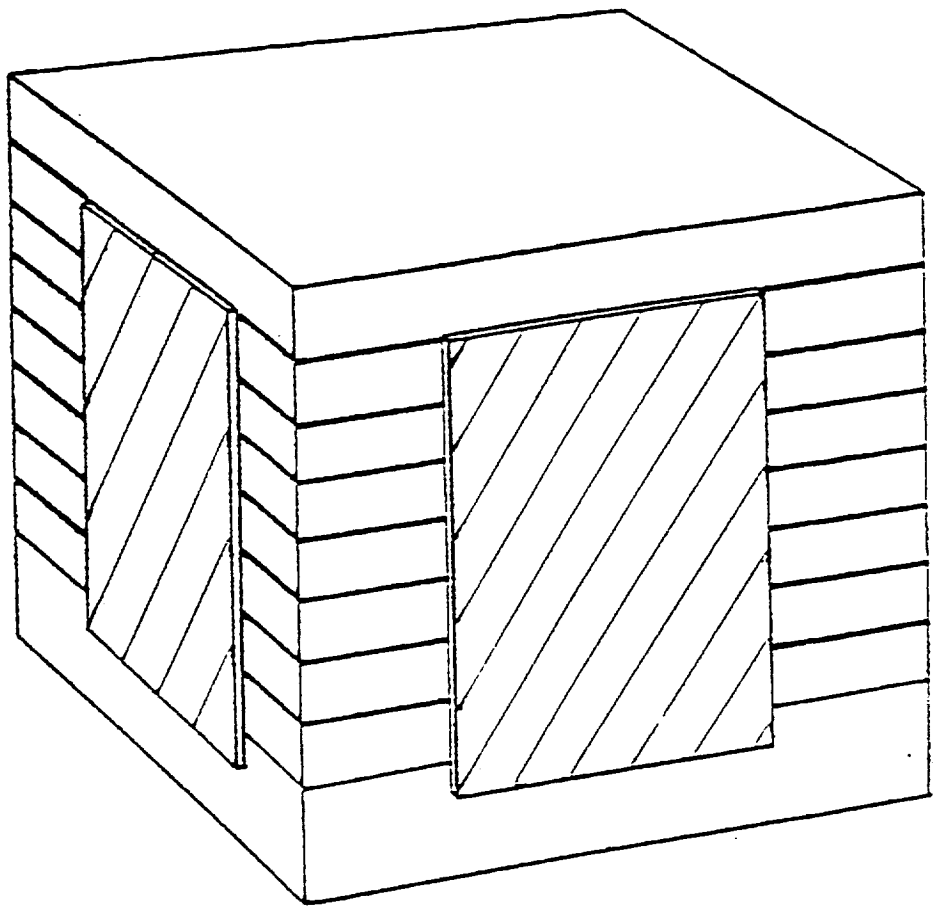

Figure 2: The detector stack, which is 4.5" square, 4.0" high, and weighs 7.25 lbs. (including aluminum container), consists of nine detector modules stacked atop each other and four additional modules attached to the sides.

TABLE 1

Assembly Dates: 6 January 1984; 16, 17 January 1984 LDEF

P0006 LINEAR ENERGY TRANSFER SPECTRUM MEASUREMENT EXPERIMENT (LETSME)

Date

1-6-84 TLD Plates -- 5 each

TLD-200 18 chips each per plate
TLD-700
Total: 90 chips each type
Batch #1 TLDs

1-6-84 Neutron Detectors

Plate 1
^{6}LiF/CR-39 (4), 2 with Gd foils
Mica/Bi/Mica (2)
Mica/Ta/Mica (3)

Plate 2
Mica/^{238}U/Mica (6)
Mica/^{232}Th/Mica (6)

1-16, 17-1984 Stack Assembly

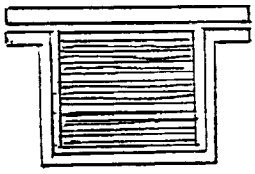

Stack begins at bottom
(actual top of the flight container).
Layers scribed on upper surface at edge.

Material	No.of Sheets	Scribed
TLD plate #1		
CR-39	(2)	7-1C, 7-2C [1BD*, 2BD]**
Melinex	(8)	3M -- 10M
Tuffak	(8)	11R -- 18R
Sheffield	(14)	19G -- 32G
Mica	(2)	33T -- 34T
Aℓ plate		

**Inserted in milled-out centers of large CR-39 sheets
*BD indicates Berkeley DOP CR-39

CR-39	(2)	7-35C, 7-36C [35BD, 36BD]
Melinex	(8)	37M -- 44M
Tuffak	(8)	45R -- 52R
Sheffield	(10)	53G -- 62G
TLD plate #2		
Aℓ plate		
CR-39	(2)	7-63C, 7-64C [63BD, 64BD]
Melinex	(8)	65M -- 72M
Tuffak	(8)	73R -- 80R
Sheffield	(10)	81G -- 90G
Aℓ plate		
CR-39	(2)	7-91C, 7-92C [91BD, 92BD]
Melinex	(8)	93M -- 100M
Tuffak	(8)	101R -- 108R
Sheffield	(10)	109G -- 118G
Aℓ plate		
TLD plate #3		
CR-39	(2)	7-119C, 7-120C [119BD, 120BD]
Melinex	(8)	121M -- 128M
Tuffak	(8)	129R -- 136R
Sheffield	(10)	137G -- 146G
Aℓ plate		
CR-39	(2)	7-147C, 7-148C [147BD, 148BD]
Melinex	(8)	149M -- 156M
Tuffak	(8)	157R -- 164R
Sheffield	(10)	165G -- 174G
Aℓ plate		
TLD plate #4		
CR-39	(2)	7-175C, 7-176C [175BD, 176BD]
Melinex	(8)	177M -- 184M
Tuffak	(8)	185R -- 192R
Sheffield	(10)	193G -- 202G
Aℓ plate		

CR-39	(2)	7-203C, 7-204C [203BD, 204BD]
Melinex	(4)	205M -- 208M
Tuffak	(4)	209R -- 212R
Sheffield	(2)	213G, 214G
Mica	(2)	215T, 216T
Melinex	(2)	217M, 218M
Tuffak	(2)	219R, 220R
Sheffield	(4)	221G -- 224G

TLD Plate #5

CR-39	(1)	7-217C

Si (3-$^{15}/_{16}$" diameter; gridded surface up)

CR-39	(1)	7-218C

Si (2" diameter; matte surface up)

CR-39	(1)	7-219C

Neutron plate (^{6}LiF, ^{209}Bi, ^{181}Ta)

Activation foils (Ni, Ta, In, V)

Neutron plate (^{238}U, ^{232}Th)

Side Stack Assembly

CR-39	(2)	A1C, A2C (and A1BD, A2BD)*
Melinex	(2)	A3M, A4M
Tuffak	(2)	A5R, A6R
Sheffield	(2)	A7G, A8G
CR-39	(2)	B1C, B2C (and B1BD, B2BD)
Melinex	(2)	B3M, B4M
Tuffak	(2)	B5R, B6R
Sheffield	(2)	B7G, B8G

*taped to large CR-39 sheet

CR-39	(2)	C1C, C2C (and C1BD, C2BD)
Melinex	(2)	C3M, C4M
Tuffak	(2)	C5R, C6R
Sheffield	(2)	C7G, C8G
CR-39	(2)	D1C, D2C (and D1BD, D2BD)
Melinex	(2)	D3M, D4M
Tuffak	(2)	D5R, D6R
Sheffield	(2)	D7G, D8G

Materials

Batch #7 CR-39 (large sheet)

Berkeley 1% DOP CR-39 (from D. Griffith)

Mica from J. H. Roberts, Westinghouse Hanford Co. (African)

Batch #1 TLDs (200 and 700)

Melinex, Tuffak, Sheffield -- first batches

Weight when assembled in aluminum container = 7.25 lb

Stack (with filter paper -- Whatman #3 -- on top and bottom) is 4 inches thick

Sheets are 4.25 inches square with corners clipped $\sim 1/16$ inch

Side stack sheets are 8 cm in vertical dimension and 5 cm in horizontal dimension

Al plates are 1/16" thick

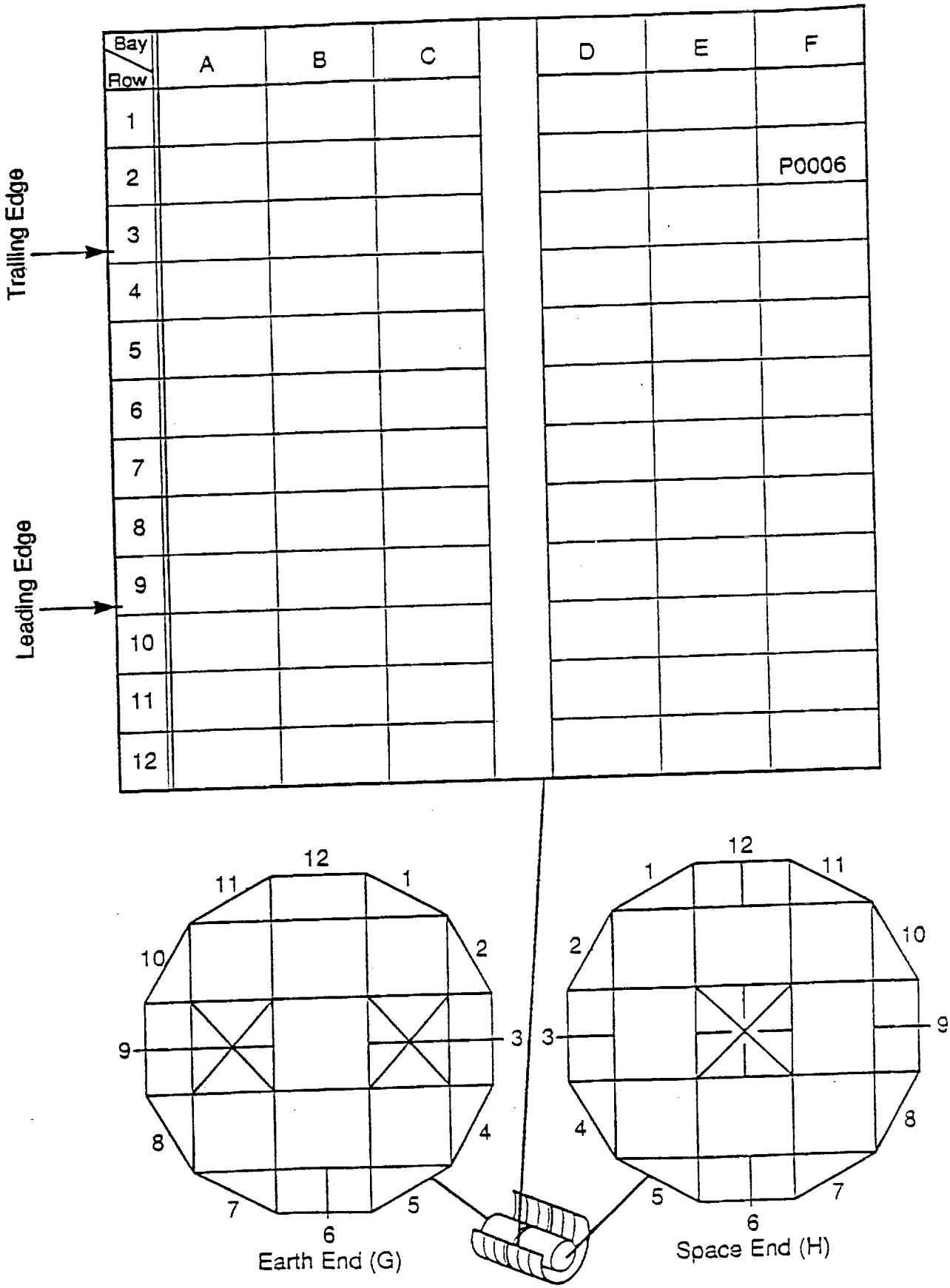

Figure 3: Location of P0006 experiment on LDEF.

Task 1: TLD Measurements

TLD Experiment

There were five plates in the large central stack containing TLDs. Each plate held 36 TLDs, 18 each of types TLD-200 (CaF_2 crystals) and TLD-700 (solid extruded ^7LiF). The dimensions of the TLDs were $0.25 \times 0.25 \times 0.035$ inches and the two types were distributed alternately over the 4.5-inch square plates. The holder plates were 0.062-inch thick acrylate with 0.375-inch diameter holes to accommodate the TLDs.

In order to accomplish the measurements, it was necessary to determine TLD calibrations valid for the duration of the mission. Two potential problems were fading of latent TLD signal over the nearly six years of the mission and the supralinearity of TLD response due to high accumulated doses.

TLD Fading Study

A study of fading in TLD-700 chips has been under way for the past 2.5 years to determine the magnitude of the fading problem. The TLDs were irradiated with 1053 mrad of ^{137}Cs γ-rays, then stored in an oven at 38°C. This temperature was projected as the highest that LDEF experiments would reach. Groups of six TLDs are removed at intervals and read out with newly irradiated TLDs of the same batch. The results up to the present time are plotted in Figure 4. It can be seen that after an initial decline in the first 6 weeks, the ratio of faded to newly irradiated doses has been approximately flat. There was no pre-heating of the TLDs so that the low temperature glow peak in LiF is included in the measurement. The initial decline comes from the decaying out of the low temperature glow peak. When pre-heating is employed (for instance by heating the TLDs to 120°C for 10 sec) the low temperature glow peak is mainly eliminated from the measurement and the response is approximately flat from the first readout. These results indicate that compensating for fading is not a serious problem in TLD-700 at temperatures under 38°C.

TLD Calibrations

The calibration TLDs were of the same batches as those used in the experiment and all were annealed together prior to the experiment. During the period of the LDEF mission, the calibration TLDs were exposed to a standard ^{137}Cs γ-ray source at two-month intervals (33 individual exposures). The mean dose was 6.284 rad (tissue equivalent) for a total dose of 207.36 rad. The purpose of this was to duplicate in the calibrations the fading of stored signal taking place in the experimental TLDs. The dose calibration factors for the TLD-200 and -700 were determined in units of rad/nC, where the TLD reader results are in units of nanocoulombs. As mentioned above, the combination of calibration exposures spread over the mission duration and preheating of the TLDs in readout assures that fading did not significantly affect the accuracy of the measurement.

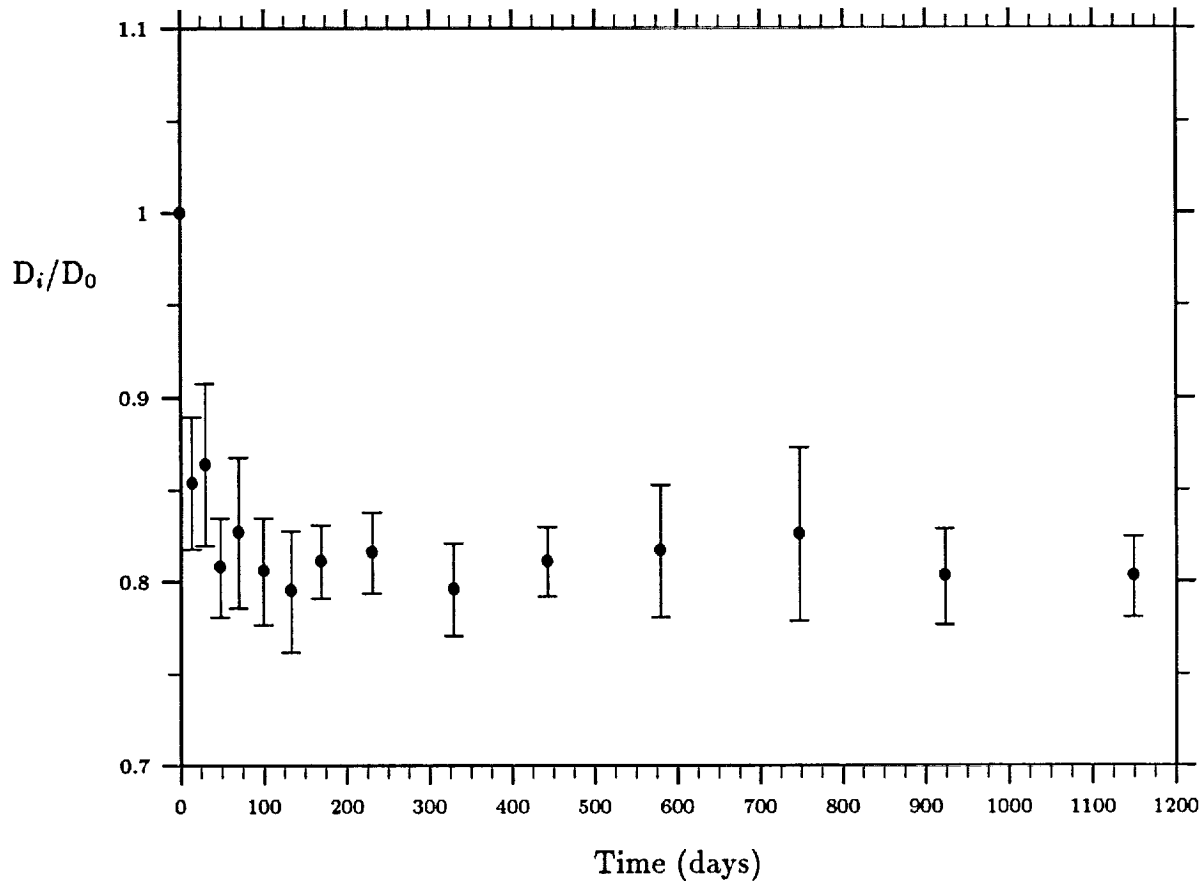

Figure 4: The fading of thermoluminescence in TLD-700 chips irradiated to 1.053 rad, then stored at 38°C, where D_i and D_0 were the doses measured on the stored TLDs and newly irradiated TLDs, respectively.

TLD High Dose Supralinearity

In calculating doses from the TLD reader integrating picoammeter measurements, it was necessary to compensate for the supralinearity of TLD response at high doses. The supralinearity becomes significant at doses of 100 rad and greater. A calibration was performed to measure this effect (see Figure 5) at the same time of the P0006 TLD readout. In this calibration, several dose points were determined with TLD-700 and a few with TLD-200 for comparison. The highest dose (10^3 rad) for the TLD-200 gave an erroneously high reading. The problem here was that, even with a 100/1 neutral density filter in place between the heated planchet and the photomultiplier tube, the TLD-200 yielded a very high light output. For TLDs of the same size, TLD-200 yields approximately 20 times the signal/dose ratio of the TLD-700. Judging from this and some previous high dose results at this laboratory, the photomultiplier tube output also becomes supralinear with respect to incident light intensity if too high a current is generated. This conclusion will be reconfirmed later. The high dose point for the TLD-200 was rejected and the dose response curve was extended from the lower dose measurements in constant relationship to the TLD-700 response.

Readout of TLDs

On 19 May 1990, the five TLD plates were removed from the stack for readout. The TLDs were read out with a Harshaw Model 4000 reader. Flight, background and calibration TLDs were read out together. Because of the high doses accumulated over the LDEF mission, a 100/1 (nominal) neutral density filter was inserted below the photomultiplier tube to reduce the light transmission from the heated TLDs. The readout cycle employed was a pre-heating at 120°C for 10 sec. followed by a 7°C/sec. heating ramp to a maximum temperature of 325°C. The current output from the photomultiplier unit was integrated between 120°C and 260°C for dose determination, but glow peaks were measured up to 325°C to examine possible dose- or LET-dependent effects.

Experimental Results from TLDs

The TLD dose measurements are given in Table 2. Mission doses are seen to vary between 266 rad (maximum shielding) and 648 rad (minimum shielding). Within the statistical uncertainty (σ) of the measurements, the TLD-200 and -700 chips gave equal readings. The standard deviations of measurement (σ) of Plates 3, 4, and 5 were not calculated directly from the spread in the individual TLD readings since their differences also included real dose differences. At the larger depths in the stack, TLDs near the sides of the canister were less shielded than those in the middle. There was a non-uniform dose across these plates. The σs were scaled from Plates 1 and 2. The minimum doses of Plates 3, 4, and 5 were about 303, 242 and 227 rad, respectively.

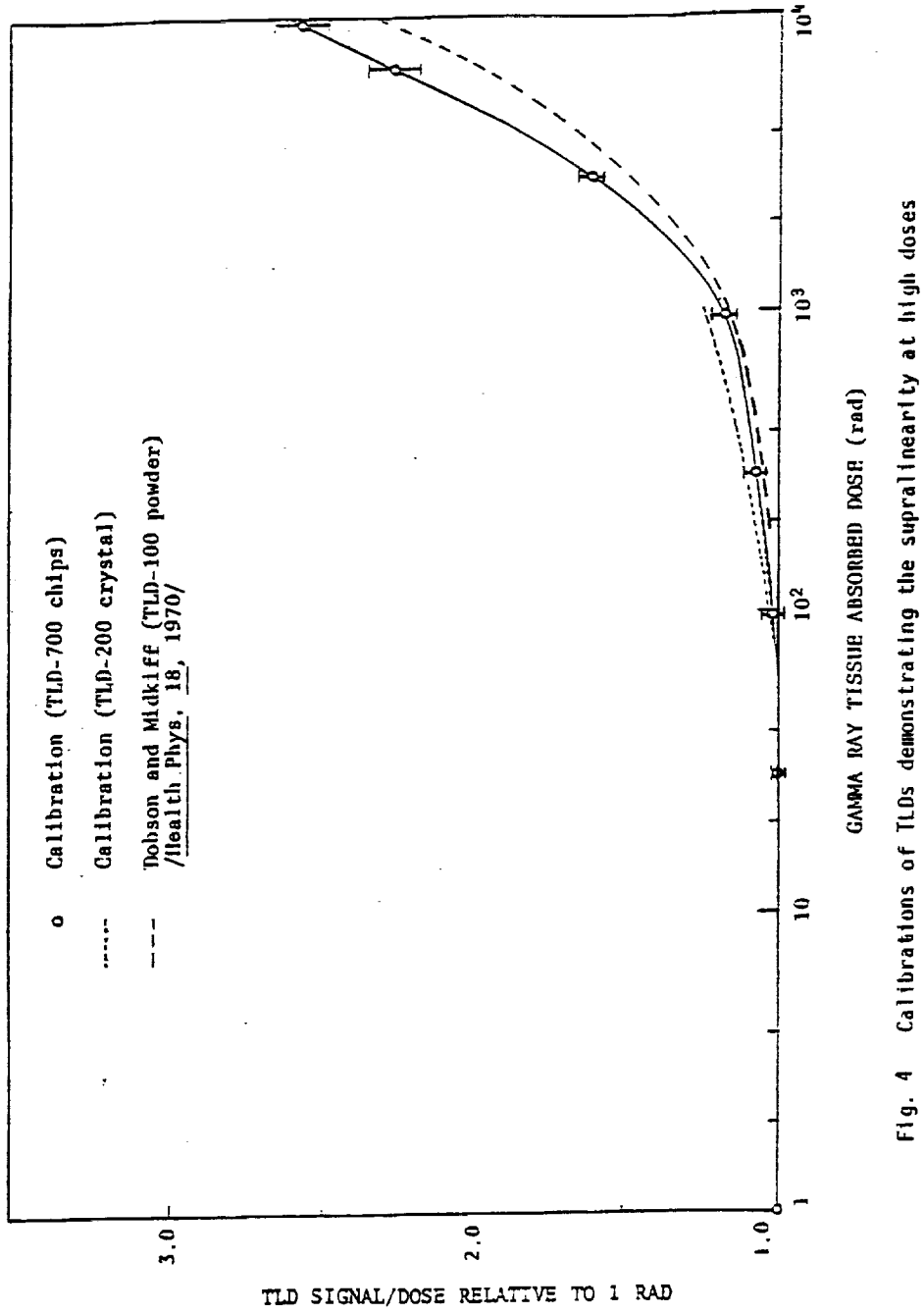

Fig. 4 Calibrations of TLDs demonstrating the supralinearity at high doses

Figure 5: Calibrations of TLDs demonstrating the supralinearity at high doses.

Table 2: P0006 TLD Measurements

TLD Plate No.	TLD Type	Tissue Absorbed Dose (rad)	Dose Rate (mrad/d)	Shielding (g/cm^2) Al	Plastic & Fiberglass	Total
1	200	628 ± 21	297 ± 10	0.446	0.561	1.01
	700	648 ± 24	307 ± 11			
2	200	392 ± 21	185 ± 10	0.918	3.04	3.96
	700	392 ± 21	185 ± 10			
3	200	320 ± 15	151 ± 7	2.20	5.38	7.58
	700	316 ± 15	149 ± 7			
4	200	282 ± 13	133 ± 6	3.05	7.74	10.8
	700	276 ± 13	131 ± 6			
5	200	273 ± 12	129 ± 6	3.53	9.87	13.4
	700	266 ± 12	126 ± 6			

The doses were approximately uniform over Plates 1 and 2 and were non-uniform over Plates 3, 4 and 5 (due to lesser shielding through the sides than through the top for the deeper TLD plates). The minimum shielding to the side (canister only) for the individual TLDs was 0.64 g/cm^2 Al plus 1.06 to 4.84 g/cm^2 plastic.

Discussion of TLD Results

The average tissue absorbed dose rates measured in the P0006 canister during the LDEF mission varied from a maximum of 307 ± 11 mrad/d under 0.464 g/cm^2 shielding to a minimum of 126 ±4 mrad/d under 12.9 g/cm^2. In comparison with measurements from other LDEF experiments there is close agreement with P0004, also on the trailing edge of the orbiter, and a wide difference from M0004 which was on the leading edge. Under minimum shielding in P0004 Canister #6 the dose rate was 314 ± 14 mrad/d, while under 1.25 g/cm^2 in the M0004 #2 detector the dose rate was 122 ± 4 mrad/d. This factor of approximately 2.5 in difference was expected and is due to the directionality of the trapped protons.

Task 2: High Energy Neutron and Proton Measurements with Fission Foils

Fission Foil/Mica Experiment

The fission foil/mica detectors were located in the #8 sub-stack at the bottom (flanged end) of the canister. The fission foils were arrayed across sections of two different acrylate plates, on either side of the four activation foils. In the plate above (space side) the activation foils were ^{209}Bi, ^{181}Ta and other detectors containing ^{6}LiF. The ^{181}Ta was to one side, the ^{209}Bi was in a strip across the middle of the plate and the ^{6}LiF was to the other side. In the plate below the activation foils were the ^{238}U and ^{232}Th, each occupying a half of the plate. There were six foils each of ^{238}U and ^{232}Th (0.5" diameter), three foils of ^{181}Ta (0.75" diameter) and two foils of ^{209}Bi (1.5" by 0.5"). Muscovite mica foils were placed against each side of the fission foils to record the tracks of fission fragments emitted during the mission.

Processing of Mica Track Detectors

The mica detectors were processed in 50% HF acid at 22°F for 1 hour. Prior to the LDEF mission they had been processed for 3 hours in order to enlarge the size of the fossil tracks in the mica. The mission and fossil tracks were easily discriminated.

Readout of Mica Track Detectors

Track densities of fission fragments in the mica were counted at 200× under an optical microscope. Approximately 1000 tracks were counted on each sample except in the case of ^{181}Ta foil detectors, where the track densities were too low. The entire mica samples were scanned for these detectors. Backgrounds were counted by scanning the reverse sides of the mica flight samples. The sample densities are given in Table 3 and 4.

It can be seen that the scatter between the different samples (σ of the average) is much greater than would be expected from random scatter in a uniform field (σ of the individual samples). This shows that there were real differences between the different sample positions in the P0006 detector stack. The different track densities were due to different incident proton and neutron fluences. Incident particle fluences are affected by shielding differences through the detector stack.

Table 3: Track Densities from Fission Foil/Mica Detectors – Background Subtracted.

Fission Foil	Track (cm^2)
$^{238}U^*$	$2.80 \pm 0.10 \times 10^4$
	$2.83 \pm 0.10 \times 10^4$
	$3.12 \pm 0.11 \times 10^4$
	$3.40 \pm 0.11 \times 10^4$
	$3.40 \pm 0.11 \times 10^4$
	$3.44 \pm 0.11 \times 10^4$
	$3.59 \pm 0.11 \times 10^4$
	$3.80 \pm 0.12 \times 10^4$
	$3.86 \pm 0.12 \times 10^4$
	$4.04 \pm 0.11 \times 10^4$
	$4.04 \pm 0.11 \times 10^4$
average =	$3.48 \pm 0.42 \times 10^4$
^{209}Bi	$1.80 \pm 0.06 \times 10^3$
	$2.12 \pm 0.07 \times 10^3$
	$2.18 \pm 0.07 \times 10^3$
	$2.31 \pm 0.07 \times 10^3$
average =	$2.10 \pm 0.19 \times 10^3$

*Corrected for spontaneous fission background of 2500 cm^{-2} and 30% reduction in fission fragment emissions due to surface oxidation.

Table 4: Track Densities from Fission Foil/Mica Detectors – Background Subtracted.

Fission Foil	Track (cm^2)
^{232}Th	$1.80 \pm 0.06 \times 10^4$
	$1.96 \pm 0.06 \times 10^4$
	$1.99 \pm 0.06 \times 10^4$
	$2.01 \pm 0.06 \times 10^4$
	$2.01 \pm 0.06 \times 10^4$
	$2.10 \pm 0.06 \times 10^4$
	$2.16 \pm 0.07 \times 10^4$
	$2.31 \pm 0.07 \times 10^4$
	$2.34 \pm 0.07 \times 10^4$
	$2.53 \pm 0.08 \times 10^4$
	$2.75 \pm 0.08 \times 10^4$
	$2.90 \pm 0.08 \times 10^4$
average =	$2.24 \pm 0.32 \times 10^4$
^{181}Ta	61.4 ± 5.3
	66.4 ± 5.4
	67.4 ± 5.4
	69.9 ± 5.6
	72.5 ± 5.6
	91.2 ± 6.3
average =	71.1 ± 9.5

Calculations from Fission Foil Measurements

The nuclei in the heavy element foils used in these measurements can undergo fissions due to collisions with either neutrons or protons of sufficient energy. The cross sections for energies up to 100 GeV are given in Figure 6. The data used to determine the cross sections over this wide range were taken from Lomanov *et al.* (1979), Wollenberg and Smith (1969) and Stehn *et al.* (1965).[6,8,7] The available data was extrapolated, where necessary, up to 100 GeV.

Calculations of neutron and proton fluence spectra accumulated from the various sources during the LDEF mission have been made by Armstrong and Colborn (1990).[1] Their data for 10 g/cm^2 Al shielding have been extrapolated, where necessary, to cover energies up to 100 GeV and then summed into total composite neutron and proton fluence spectra (Figure 7). The graph extends over 5 decades in energy and more than 8 decades in fluence. Summations of these energy spectra yield values of 7.5×10^8 neutrons/cm^2 (1 MeV–100 GeV) and 1.09×10^9 protons/cm^2 (10 MeV–100 GeV) for the total integrated LDEF fluences. Due to our handling of the data these numbers may be a few percent different from comparable values derived by the authors of the original calculations.

The neutron and proton energy spectra together with the fission cross sections can be used to calculate the fission fragment track densities expected from the fission foil/mica detectors. The numerical integration is

$$D = \epsilon \sum_{E_{min}}^{E_{max}} \sigma_F(E) N(E), \qquad (1)$$

where D is track density, ϵ is track registration efficiency for the foil material ($\epsilon = 1.16 \times 10^{-5}$ tracks/n-b), σ_F is the fission cross section in barns and N is the differential fluence (cm^{-2} MeV^{-1}) of neutrons and protons.

Results from Fission Foil Measurements

The calculated and measured fission foil track densities are compared in Table 5. The calculated total track densities are all less than the measured average. The ratio varies between 0.80 and 0.61 for ^{238}U, ^{232}Th, and ^{209}Bi but for ^{181}Ta it is 0.46. The greater difference for ^{181}Ta could be due to the high energy extrapolations made in determining the spectra and cross sections. Only the ^{181}Ta foil calculations result in a large fraction of total tracks being produced by nucleons above 1 GeV.

A second item of interest from Table 5 is the fraction of the total calculated track density due to neutrons. The fraction varies from 0.11 to 0.28 with ^{209}Bi and ^{181}Ta being particularly low in neutron efficiency. This means that the neutron spectrum, particularly at the higher energies, could vary in fluence by a large amount with a moderate change in total track density. As an example the difference seen between calculated and measured track densities

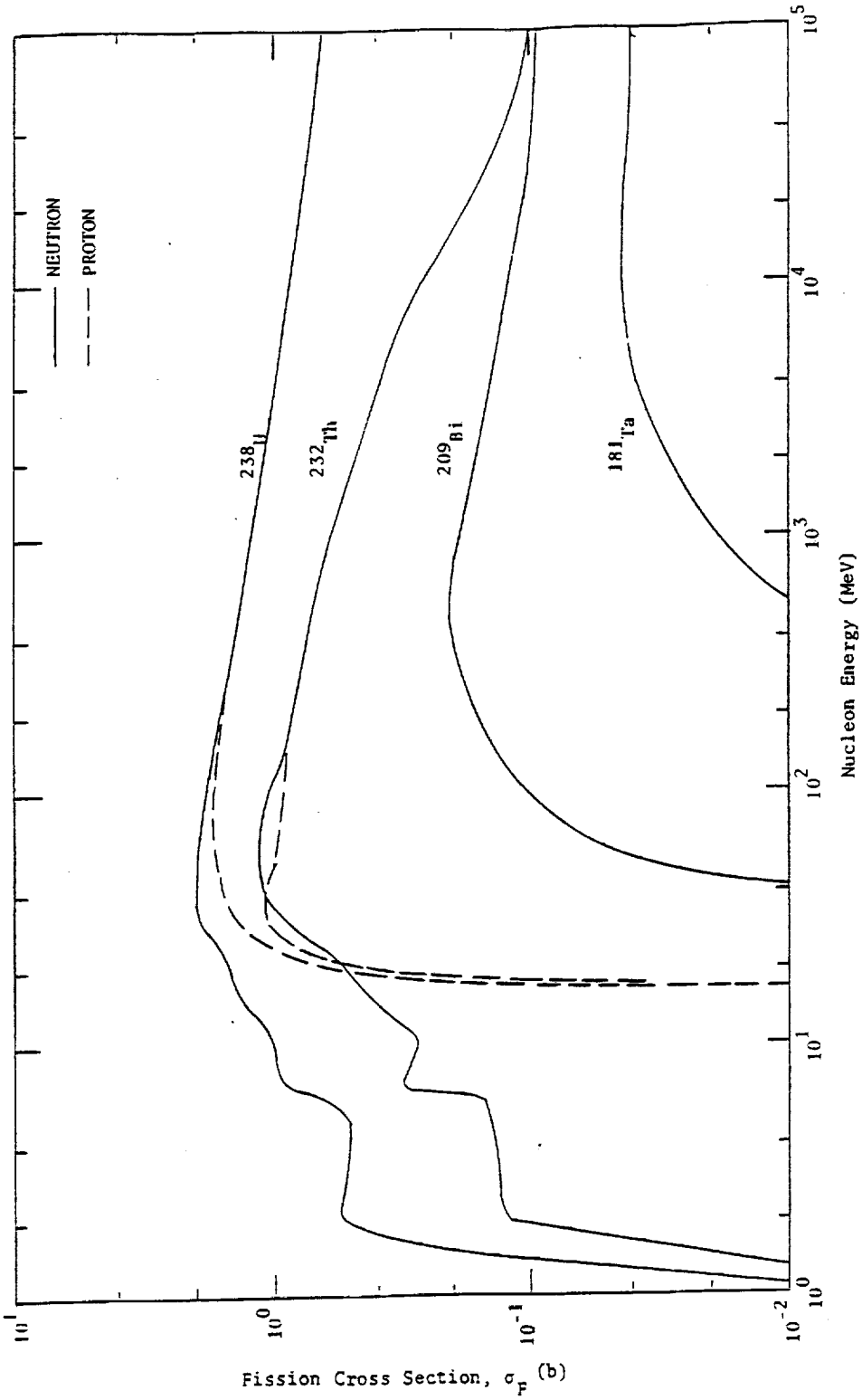

Figure 6: Fission cross sections for neutrons and protons incident on heavy metal foils.

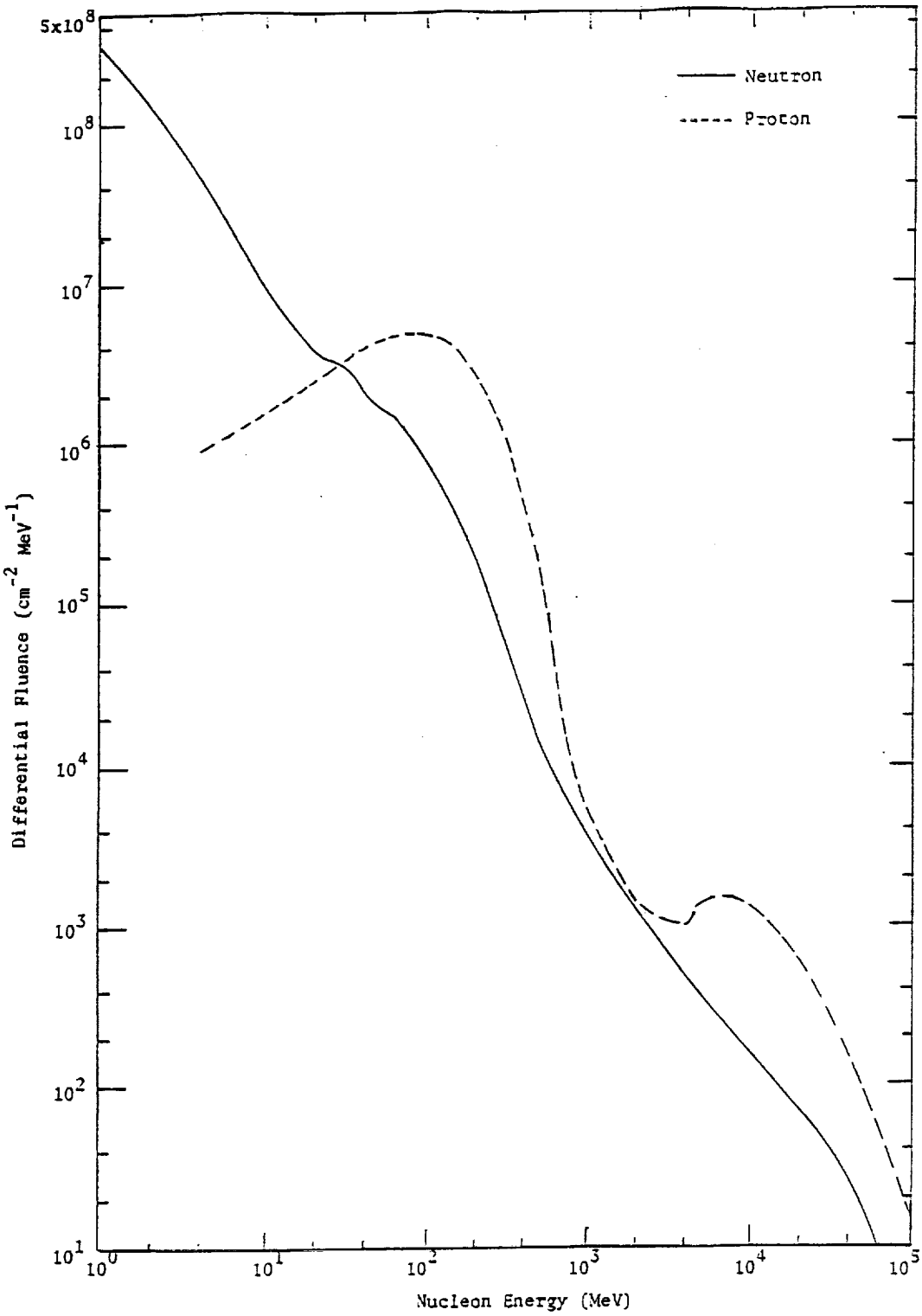

Figure 7: Differential spectra of neutrons and protons accumulated during the total LDEF mission under 10g/cm^2 Al. From data by Armstrong and Colborn (1990). Summations and extrapolations by authors.

Table 5: Results of the Fission Foil/Mica High Energy Neutron Detectors.

Fission Foil	Calculated neutron (tracks/cm^2)	Calculated proton (tracks/cm^2)	Calculated total (tracks/cm^2)	Measured average (tracks/cm^2)
^{238}U	7.51×10^3	1.97×10^4	2.72×10^4	$3.48 \pm 0.42 \times 10^4$
^{232}Th	3.07×10^3	1.06×10^4	1.37×10^4	$2.24 \pm 0.32 \times 10^4$
^{209}Bi	1.84×10^2	1.50×10^3	1.68×10^3	$2.10 \pm 0.19 \times 10^3$
^{181}Ta	4.38	28.5	32.9	71.5 ± 9.5

for the ^{238}U, ^{232}Th and ^{209}Bi foils would be approximately compensated if the calculated LDEF neutron fluence was 3 times as great.

The spread in the measured track densities for the several detectors of each foil type are due at least in part to differences in shielding. Table 6 summarizes the minimum shielding of the detectors through the top and side of the flight canister and detector stack. It should be remembered in looking at the minimum shielding that the total side-to-side mass thickness of the detector stack is 13.5 g/cm^{2}plastic. Since the different fission foils occupy restricted areas of layers in the stack, the minimum shielding for each type extends in different direction or directions. The directionality of incident radiation can therefore also contribute to a spread in measurements, both within a foil set and between foil types.

The proton absorbed dose and neutron dose equivalent can be determined from the calculated spectra. The measured and calculated track densities for the fission foil detectors can then be used to find the doses consistent with the experimental measurements. This assumes that the relative intensities of the calculated proton and neutron spectra reflect the experimental conditions. The proton dose is given by

$$D = (1.602 \times 10^{-8}) \sum_{E_1}^{E_2} N(E) \frac{dE}{dx}(E) \text{ rad}, \tag{2}$$

where E_1 and E_2 are 10 MeV and 100 GeV, $N(E)$ is the differential proton spectrum in cm^{2}MeV^{-1} and $\frac{dE}{dx}$ is the energy absorption of protons in tissue in MeVcm^2/g.

The dose equivalent for neutrons is given by

$$DE = 10^{-3} \sum_{E_1}^{E_2} d(E) N(E) \text{ rem}, \tag{3}$$

where E_1 and E_2 are 1 MeV and 60 GeV, $d(E)$ is the dose equivalent conversion factor in mrem·cm^2 and $N(E)$ is the differential neutron spectrum in cm^{-2}MeV^{-1}. The d values were taken from NCRP (1971) up to 500 MeV and extended up to 60 GeV from that energy.

Table 6: Minimum Shielding of the Fission Foil Detectors through the Top and Side of the Flight Package.

Minimum Detector Shielding (g/cm^2)

Top

	Plastic*	Al	Si (average)	Ni, Ta, In, V Range	Ni, Ta, In, V Average	Total (average)
^{238}U	10.6	3.5	0.12	3.9–10.5	6.2	20.4
^{232}Th	10.6	3.5	0.12	3.9–10.5	6.2	20.4
^{209}Bi	10.4	3.5	0.12	—	—	14.0
^{181}Ta	10.4	3.5	0.12	—	—	14.0

Side (Canister Only)

	Plastic Range	Plastic Average	Al	Total (average)
^{232}U	1.1–6.8	4.0	0.64	4.6
^{232}Th	1.1–6.8	4.0	0.64	4.6
^{209}Bi	1.2–6.0	3.6	0.64	4.2
^{181}Ta	1.9–3.9	2.9	0.64	3.5

*Includes 0.5 g/cm^2 fiberglass.

Table 7: High Energy Proton and Neutron Doses

	Proton Tissue† Absorbed Dose (rad)	Proton Dose† Rate (mrad/d)	Neutron Dose‡ Equivalent (rem)	Neutron Dose‡ Equiv. Rate (mrem/d)
Calculated*	142	67	33.1	15.7
Measured**	197	93	46	22

*For proton energy range of 10 MeV to 100 GeV and neutron range of 1 MeV to 60 GeV. Proton and neutron spectra derived from data by Armstrong and Colburn (1990) for 10 g/cm^2 Al shielding.
**Determined by adjusting calculated doses for difference between calculated and measured track densities for ^{238}U, ^{232}Th, and ^{209}Bi fission foil detectors.
†Proton energy range of 10 MeV to 100 GeV.
‡Neutron energy range of 1 MeV to 60 GeV.

The doses are given in Table 7. The effective QF for the neutron spectrum was 8.4 and the effective d was 4.42×10^{-5} mrem·cm^2. Doses which are consistent with the measured track densities have been determined by assuming that the relative spectral distributions of the calculated protons and neutrons are correct for the experimental spectra and only the absolute magnitude changes. The proton dose should compare well with the doses from the more heavily shielded TLDs in the P0006 experiment. From the TLD doses in Table 2 it can be seen that agreement with the calculated proton dose is quite close. The proton dose derived from the fission foil measurements is higher and corresponds to TLD doses which have less shielding than did the fission foils.

The neutron dose equivalents from P0006 can be compared to measurements from other space missions. The Cosmos 936 (incl. = 62.8°, alt. = 419/224 km) and 1129 (incl. = 62.8°, alt. = 394/226 km) experiments included similar sets of fission foils inside the spacecraft. Dose equivalent rates of 6.8 mrem/d were measured on each mission, which were less than the 15.7 mrem/d (calculated) and 22 mrem/d (measured) on LDEF. However the ratio of high energy neutron dose equivalent to total absorbed dose rate (from TLDs) were 0.27 and 0.38, respectively, on the two Cosmos missions and was 0.35 for the P0006 experiment. As a fraction of incident charged particle dose, the neutron dose equivalents were in better agreement for these different orbits and shielding distributions. Because of different neutron contributions from primary charged particle production and albedo from the earth's atmosphere, as well as shielding differences, these ratios should be expected to vary. On Cosmos 2044 (incl. = 82.3°, alt. = 294/216 km) a set of ^{232}Th foils, mounted outside the

spacecraft, yielded 3.3 mrem/d.

Discussion of Fission Foil Measurements

The calculated fission foil track densities (10 g/cm^2 Al shielding) for the LDEF mission are less than the average measured by 22% (^{238}U), 39% (^{232}Th), 20% (^{209}Bi) and 54% (^{181}Ta). Because of the complex shielding and directional experimental environment it is not possible to attach significance to these differences. An overall difference between calculation and experiment of a factor of 2 would indicate reasonable agreement under these conditions. Since the majority of the calculated tracks are induced by protons, an approximate agreement with the calculated total proton spectrum is indicated by the measurements. This agreement between experiment and the calculated spectra is substantiated by a dose of 142 rad found for the calculated proton spectrum and which is fairly close to the TLD doses measured under comparable shielding (Table 2). The neutrons contribute a smaller portion of the tracks so less can be said about agreement between measurements and the calculations. Agreement within a factor of 5 is indicated.

Task 3: Thermal and Resonance Neutron Measurements with ^{6}LiF/CR-39 Detectors

^{6}LiF/CR-39 Experiment

The ^{6}LiF/CR-39 detectors were located in the #8 sub-stack at the bottom (flanged end) of the canister, and within the same acrylate plate as the ^{181}Ta and ^{209}Bi fission foils. Two detectors without Gd foil (0.0025" thickness) covers were alternated with two detectors with Gd covers. The four detectors were placed in a row along one side of the acrylate plate.

^{6}LiF foils were 4.5 mg/cm^{2} thick on a heavy paper back of 5/8" diameter. Discs of CR-39 PNTD were placed against the ^{6}LiF to record alpha particles emitted as a result of the ^{6}LiF(n,α) T reaction. The Gd foil covers absorb out thermal neutrons so the two detector types can be used to determine thermal and resonance fluences separately.

Processing of CR-39 PNTDs

The CR-39 detectors were processed in 6.25 N NaOH solution at 70°C for 1.25 hours. This was only 25% of the standard processing time and was necessary because of the high density of tracks on the CR-39 surfaces. For longer processing times the overlapping of tracks would have become a problem.

Readout of CR-39 PNTDs

Track densities of alpha particle tracks on the detectors were counted at 430× under an optical microscope. The short stopping alpha particle tracks were discriminated from the greater part of the background tracks on the basis of larger track size. For those background tracks in the size range of the alphas, the back surfaces of the detectors were counted. The background tracks consisted of GCRs and trapped particles plus their secondaries, and also ^{3}H nuclei from the ^{6}LiF(n,α) T reaction. The track densities are given in Table 8. The standard deviations reflect the counting statistics.

Neutron Measurements

The track densities were converted to neutron fluences and dose equivalents by methods previously developed.[2] Neutrons are assumed to be thermalized below 0.2 eV (the effective Gd foil energy cutoff) and to follow an $1/E_n$ energy distribution between 0.2 eV and 1 MeV. The errors introduced by these assumptions cannot be determined but probably fall within ±20% for the thermal neutrons and ±50% for the resonance neutrons. The dose equivalents were determined from the fluences using dose conversion factors from NCRP (1971) which incorporated QF values of 2 for thermal neutrons and 6.4 for resonance neutrons. The fluences and dose equivalents are given in Table 9.

Table 8: Track Densities from the ^{6}LiF/CR-39 Detectors - Background Subtracted.

Detector No.	Gd Foil	Track Density (cm^{-2})	Average Density (cm^{-2})
1	No	$10.30 \pm 0.028 \times 10^5$	9.64×10^4
2	No	$8.97 \pm 0.18 \times 10^4$	
3	Yes	$3.64 \pm 0.14 \times 10^4$	3.66×10^4
4	Yes	$3.67 \pm 0.12 \times 10^4$	

Table 9: Thermal and Resonance Neutron Measurements

Neutron Energy Range	Neutron Fluence (cm^{-2})	Dose Equivalent (mrem)	Dose Equiv. Rate (mrem/d)
$E_n \leq 0.2$ eV	$1.22 \pm 0.24 \times 10^7$	1.24 ± 2.4	$5.9 \pm 1.1 \times 10^{-3}$
0.2 ev $< E_n <$1 MeV	$1.43 \pm 0.72 \times 10^8$	700 ± 350	0.33 ± 0.16

Minimum shielding above the detector was 10.6 g/cm^2 plastic, 3.5 g/cm^2 Al, 0.12 g/cm^2 Si (ave.) and a total of 14.0 g/cm^2. Minimum shielding to the side of the detectors was 2.1 g/cm^2 plastic, 0.64 g/cm^2 Al and a total of 2.74 g/cm^2 plus shielding external to the flight canister.

Discussion of ^{6}LiF/CR-39 Results

The thermal and resonance neutron dose equivalents can be compared to other measured values on LDEF and on other orbital missions. The total dose equivalent rate of 0.34 mrem/d is a small fraction of the P0006 TLD dose rate (126 mrad/d in TLD plate #5) and also less than the high energy neutron dose equivalent rate (22 mrem/d). In comparison with thermal and resonance dose equivalent rates from other flights, on the Cosmos 936 and 1129 missions values of 0.34 and 0.43 mrem/d were measured inside the spacecraft. The mission orbits had altitudes of 419/224 km and 394/226 km, respectively, and inclinations of 62.8°. Measurements outside the spacecraft on Cosmos 2044 (altitude of 294/216 km and inclination of 82.3°) yielded 0.27 mrem/d. Considering the possible errors in the measurements and the different primary particle fluences for the different orbits, these values are quite close. For short STS missions (a few days) values of 0.12 to 0.46 mrem/d were found inside the crew compartment with an average over 11 missions of 0.27 mrem/d.

Task 4: Plastic Nuclear Track Detectors

Five types of plastic nuclear track detectors (PNTDs) were included in the P0006 experiment. Two types of CR-39 were included, pure and CR-39 with DOP plasticizer. Pure CR-39 is sensitive to ionizing radiation with a minimum LET_{∞}·H_2O of ~5 keV/μm while CR-39 with DOP is somewhat less sensitive but retains a clearer surface after chemical processing. Two types of polycarbonate were included, Tuffak and Sheffield, and are sensitive to a minimum LET_{∞}·H_2O of ~250 keV/μm. Melinex polyester was the least sensitive PNTD to be included in the P0006 experiment with a minimum registration LET_{∞}·H_2O of ~350 keV/μm.

Determination of Processing Duration

Due to the unprecedented length of the LDEF mission, the track fluence in the CR-39 detectors aboard LDEF was anticipated to be very high. CR-39 track detectors become saturated at a fluence of approximately 10^5 tracks/cm^2. CR-39 detectors flown on a typical STS mission are usually processed for 168 hours at 50°C in a solution of 6.25 *N* NaOH. For the LDEF CR-39 PNTDs, these etch conditions would lead to severe over-etching, resulting in overlapping and indistinguishable tracks. Samples of P0006 CR-39 were etched for a variety of time durations at 50°C in 6.25 *N* NaOH in order to determine the optimal etch conditions.

Etch of P0006 CR-39 detectors was carried out for period of 24, 36, 48, and 168 hours respectively. After etching, the detectors were measured under an optical microscope and the fluences of single surface and two surface tracks were measured. Table 10 lists the single surface fluences, etch times and bulk etch of the preliminary test etch detectors. The surface of the CR-39 detector processed for 168 hours was over-etched and the elliptical dimensions of the tracks could no longer be accurately measured. The fluences on the CR-39 test etch detectors were comparable to one another and determination of etch time was based on track size and ability to measure the track parameters. The samples were evaluated to determine which processing duration produced detectors which could be most easily and accurately measured. For P0006 CR-39 PNTDs, a period of 36 hours was found to be optimal.

A similar procedure was used to determine the etch durations for the polycarbonate PNTDs. Samples of P0006 polycarbonate PNTDs were etched for 24, 48, and 96 hours respectively. The fluences of single surface tracks on the Tuffak and Sheffield materials were measured. Table 11 list the fluence, etch duration and bulk etch for the polycarbonate test etch samples. As with the CR-39 test etch samples, little variation in fluence was seen as a function of etch duration. An evaluation was made as to ease and accuracy of locating

Table 10: Fluences and Etch Parameters of P0006 CR-39 Test Etch Samples.

Sample Name	Etch (hours)	Bulk Etch (μm)	Fluence (tracks/cm^2)
7-204-C1 (top)	24	4.99	$1.5 \pm 0.04 \times 10^5$
7-204-C1 (bottom)	24	4.99	$1.0 \pm 0.02 \times 10^5$
7-204-C2 (top)	168	40.2	$1.5 \pm 0.03 \times 10^5$
7-204-C2 (bottom)	168	40.2	$1.3 \pm 0.03 \times 10^5$
7-204-C3 (top)	48	15.4	$2.1 \pm 0.05 \times 10^5$
7-204-C3 (bottom)	48	15.4	$1.5 \pm 0.03 \times 10^5$
7-204-C4 (top)	36	9.53	$1.4 \pm 0.03 \times 10^5$
7-204-C4 (bottom)	36	9.53	$0.72 \pm 0.02 \times 10^5$

and measuring tracks on the polycarbonate surface. Extrapolating from etch time and track size, an etch of 144 hours was deemed optimal.

Environmental Effects on Latent Tracks in PNTDs

In support of the P0006 experiment, numerous ground based studies have been carried out to ascertain the effect of long duration storage at elevated temperatures on latent particle tracks in the various PNTD materials. Full details of these studies may be found in USF-TR-78.[5] Results of these studies were used in analysis and interpretation of LDEF data. All of the studies were carried out at a temperature of 38°C. The temperature profile of the first year of the LDEF mission indicates that the temperature seldom reached 38°C and then only for very short intervals of time.[3]

Detectors of Sheffield and Tuffak polycarbonate showed an initial decrease in reduced etch rate, $V_R - 1$, during the first several months of storage at 38°C in air. $V_R - 1$ then remained fairly constant through a period of 21 months. Samples of Sheffield and Tuffak polycarbonate were exposed behind a brass wedge to a beam of 570 MeV/amu Ar. Figure 8 shows $V_R - 1$ for the polycarbonates as a function of storage time at 38°C.

In processing the Tuffak and Sheffield polycarbonate detectors from the P0006 flight and ground control packages, all detectors were stored in air at ambient temperature for a minimum period of two months before chemical processing. In addition, those detectors exposed to heavy ion beams for calibration purposes were also stored for two months in air at ambient temperature. Thus time for the initial fading in track signal has been allowed for in both experimental flight and ground control detectors and calibration detectors.

Little change in $V_R - 1$ was seen for Melinex polyester. Figure 8 shows $V_R - 1$ as a function of storage time in air at 38°C. Samples of Melinex polyester were also exposed behind a brass

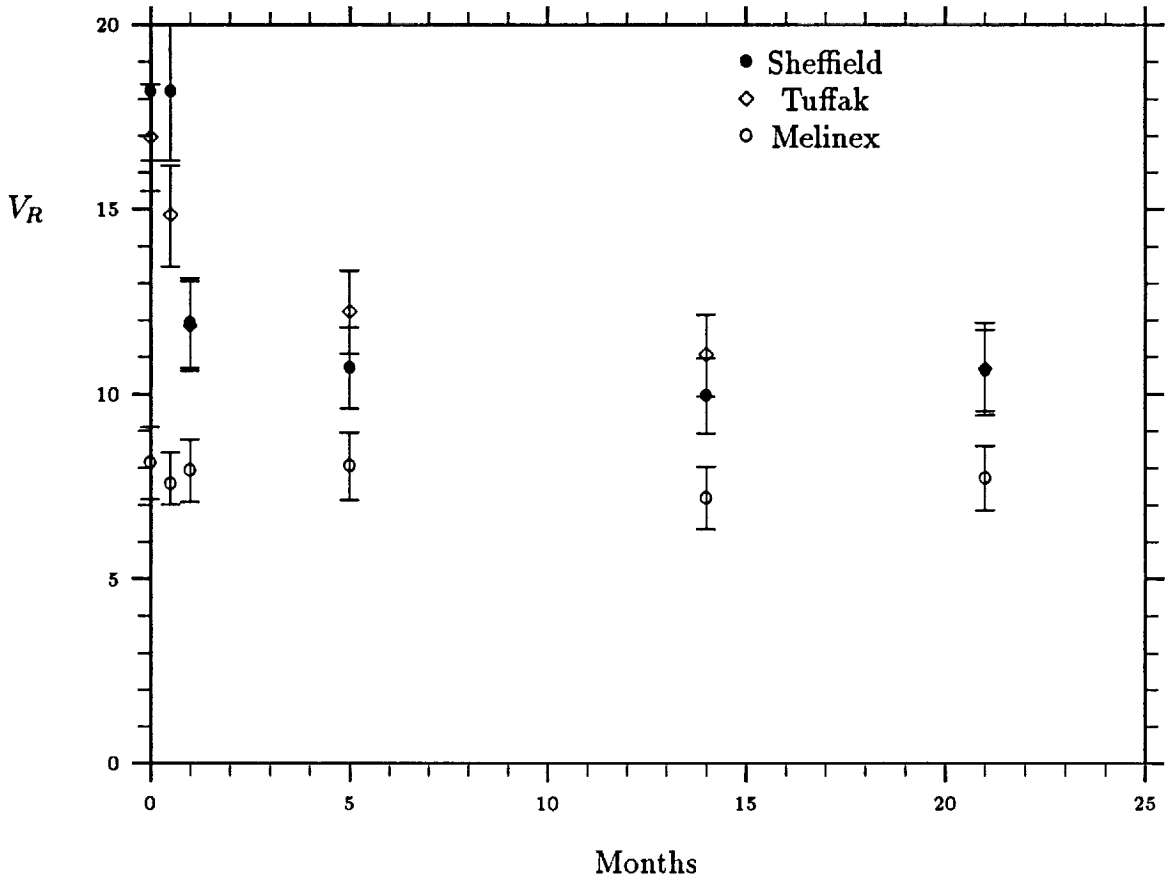

Figure 8: $V_R - 1$ as a function of Annealing Time at 38°C for 570 MeV/amu Ar ions in Sheffield, Tuffak, and Melinex. For the Sheffield and Tuffak polycarbonates, there is an initial decrease in $V_R - 1$ during the first two months of annealing, after which $V_R - 1$ plateaus. $V_R - 1$ for the Melinex polyester stays constant, within experimental uncertainty, through 21 months of annealing.

Table 11: Fluences and Etch Parameters of P0006 Polycarbonate Test Etch Samples.

Sample Name	Material	Etch (hours)	Bulk Etch (μm)	Fluence (tracks/cm^2)
213G1 (top)	Sheffield	24	4.75	$3.6 \pm 0.08 \times 10^3$
213G1 (bottom)	Sheffield	24	4.75	$3.2 \pm 0.07 \times 10^3$
213G2 (top)	Sheffield	96	21.5	$8.3 \pm 0.19 \times 10^3$
213G2 (bottom)	Sheffield	96	21.5	$7.0 \pm 0.16 \times 10^3$
213G3 (top)	Sheffield	48	15.6	$6.9 \pm 0.15 \times 10^3$
213G3 (bottom)	Sheffield	48	15.6	$6.4 \pm 0.15 \times 10^3$
212R1 (top)	Tuffak	24	6.41	$4.1 \pm 0.09 \times 10^3$
212R1 (bottom)	Tuffak	24	6.41	$3.1 \pm 0.07 \times 10^3$
212R2 (top)	Tuffak	96	22.6	$10.3 \pm 0.23 \times 10^3$
212R2 (bottom)	Tuffak	96	22.6	$8.1 \pm 0.18 \times 10^3$
212R3 (top)	Tuffak	48	15.5	$8.5 \pm 0.19 \times 10^3$
212R3 (bottom)	Tuffak	48	15.5	$6.7 \pm 0.15 \times 10^3$

wedge to 570 MeV/amu Ar.

Numerous studies were made with CR-39 PNTD. Details of the particular studies may be found in USF-TR-78.[5] All studies in CR-39 were carried out in an oven at a constant temperature of 38°C, in air. CR-39 detectors were exposed to beams of 900 MeV/amu Fe, 1.76 GeV/amu Fe, 282 MeV/amu Ne and 400 MeV/amu Ne. In these studies, the reduced etch rate V_R tended to remain fairly constant for the duration of annealing, but the bulk etch rate V_G and the track etch rate V_T both increased. Figure 9 show $V_R - 1$, V_G and V_T as functions of annealing time at 38°C and is fairly representative of the other CR-39 studies. After several months of annealing, the surfaces of CR-39 detectors deteriorated to a point where tracks were no longer measurable. It should be noted that the temperature aboard LDEF rarely approached 38°C while the annealing studies were conducted at a constant temperature of 38°C for the entire duration. The kind of surface degradation in CR-39 seen in the fading studies was not seen in any of the P0006 flight material processed thus far.

Annealing studies carried out in CR-39 with DOP plasticizer showed no change in $V_R - 1$, V_T, or V_G as functions of storage time. Samples of DOP CR-39 detector were exposed to a beam of 900 MeV/amu Fe. Storage was carried out in air at a constant temperature of 38°C. Figure 10 shows $V_R - 1$, V_T and V_G as functions of storage time. No change in the surface quality was seen during the duration of the study.

Environmental effects on latent tracks were compensated for by adjusting the calibration

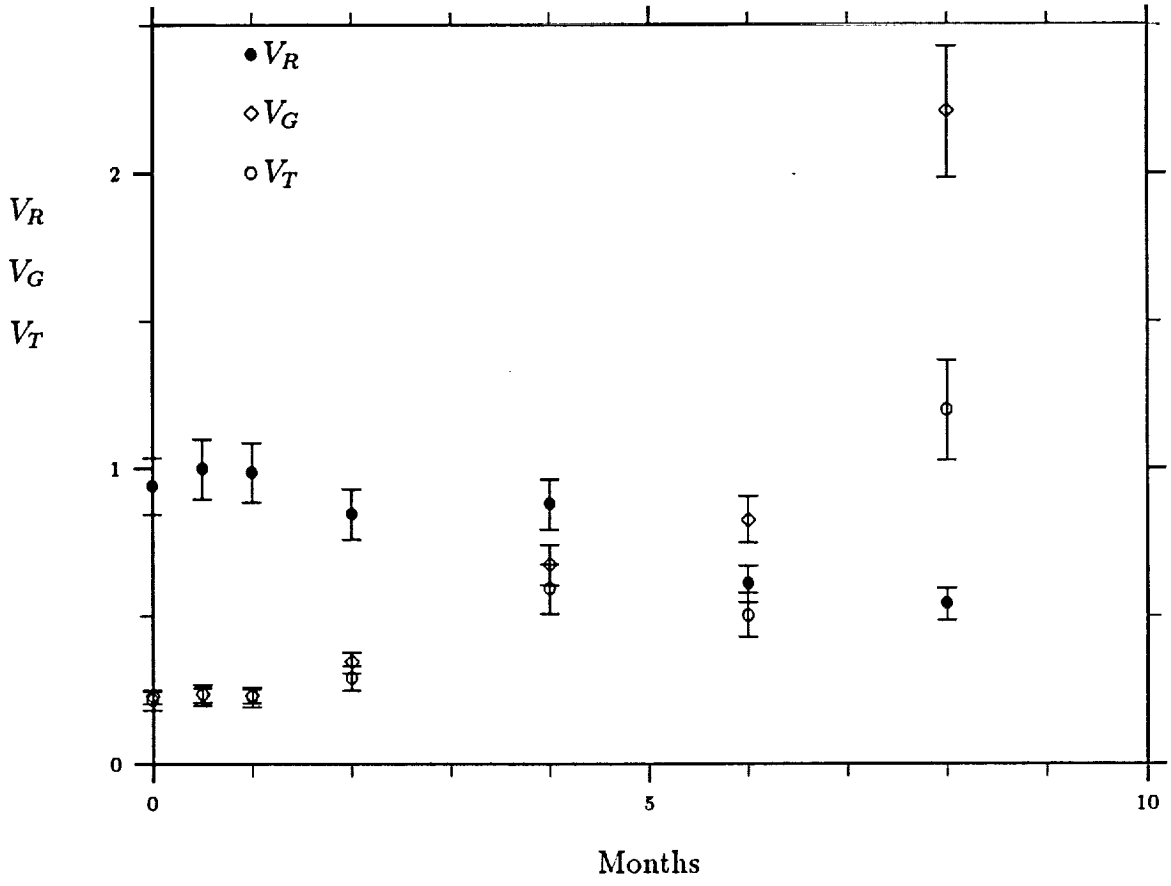

Figure 9: Etch rates as a function of Annealing Time at 38°C for 900 MeV/amu Fe, 16-U4 CR-39. Both V_T and V_G increase with annealing time. V_G increases slightly faster leading to the small decrease seen in $V_R - 1$. After 8 months of annealing, it is no longer possible to measure bulk etch B and the tracks are no longer visible on the detector.

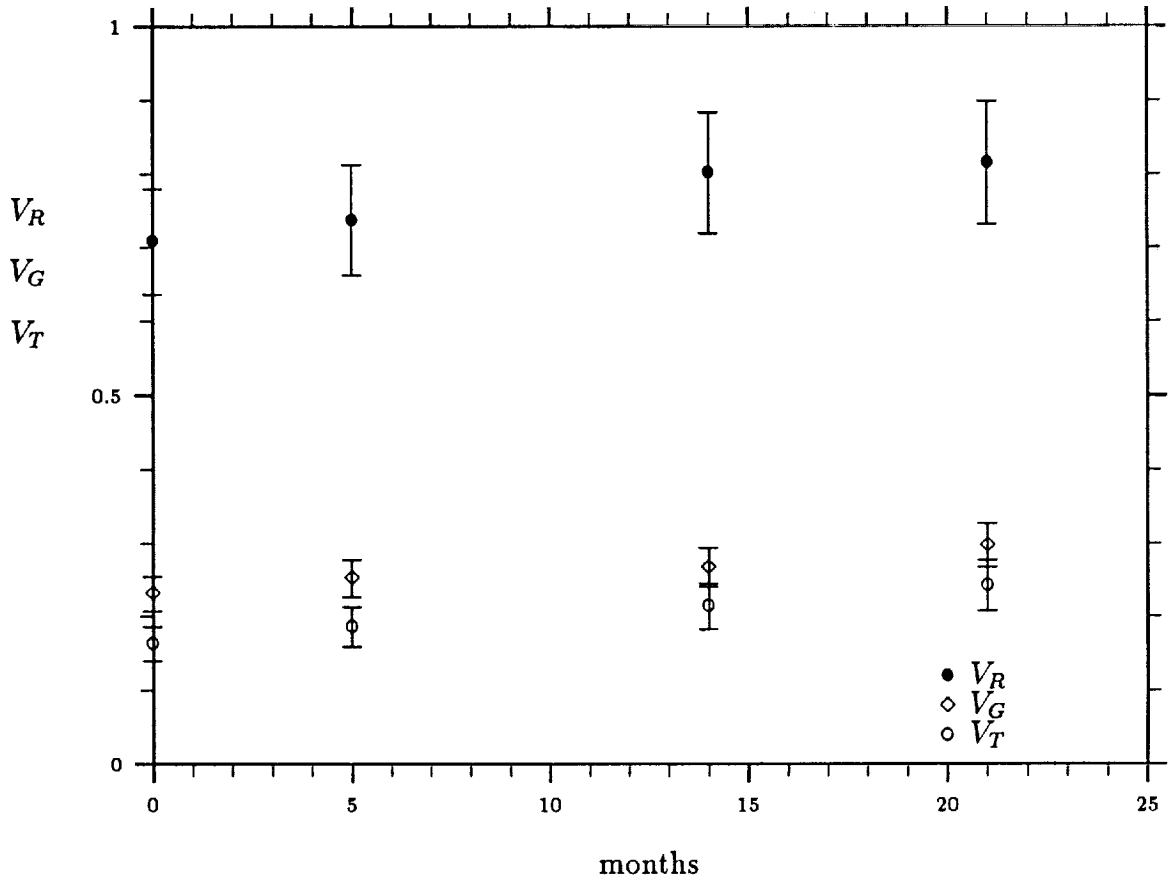

Figure 10: Etch rates as a function of Annealing Time at 38°C for 900 MeV/amu Fe, DOP CR-39. $V_R - 1$ stays constant, within experimental error for the duration of the annealing time. There is little change in either V_T or V_G.

Table 12: Summary of P0006 Calibration Irradiations at the LBL Bevalac Accelerator

Ion	Energy MeV/amu	Range (cm H_2O)	LET_∞·H_2O (keV/μm)	LET_{200}·CR-39 (keV/μm)
Kr	1367	32.3	266	179
Au	1150	12.6	1320	888
Fe	1691	54.5	136.2	91.6
U	928	8.36	1882	1266
Ag	1452	26.7	451	303

response equation for CR-39 without environmental effects by those points obtained from heavy ion accelerator exposures of P0006 flight and ground control detectors.

Calibration of PNTDs

Due to environmental changes in the sensitivity of the PNTDs and to changes in the chemical processing time, P0006 control detectors, portions of the flight material, and PNTD material of the same manufactured batches as that included in P0006 were exposed to a variety of heavy ion beams at the Lawrence Berkeley Laboratory Bevalac accelerator for purposes of calibration. The PNTDs were irradiated to ions of known energy and known LET. Table 12 is a summary of the accelerator based irradiations. Calibration detectors are scanned in order to obtain the reduced track etch rate V_R for the particular ion/energy combination. A plot of V_R versus LET is then generated for all the calibration ions and a detector response equation is found for the material.

In the case of the materials flown on LDEF, response equations already existed. However, these response equations did not take into account the environmental changes in sensitivity of the material. In addition, these response equations were for a standard chemical processing duration of 168 hours. After the irradiation of a selection of the P0006 PNTDs at the LBL Bevalac accelerator, the new calibration points (V_R, LET) were added and the response equations were adjusted to reflect this change in sensitivity. Figure 11 is the adjusted calibration plot generated for Sheffield and Tuffak polycarbonate. Figure 12 is the adjusted calibration plot generated for CR-39. The points labeled "A" are the calibration points from the 168 hour etch adjusted for change in etch duration and environmental effects. The detector response equations derived from these graphs were used to generate the LET spectra for the P0006 detectors.

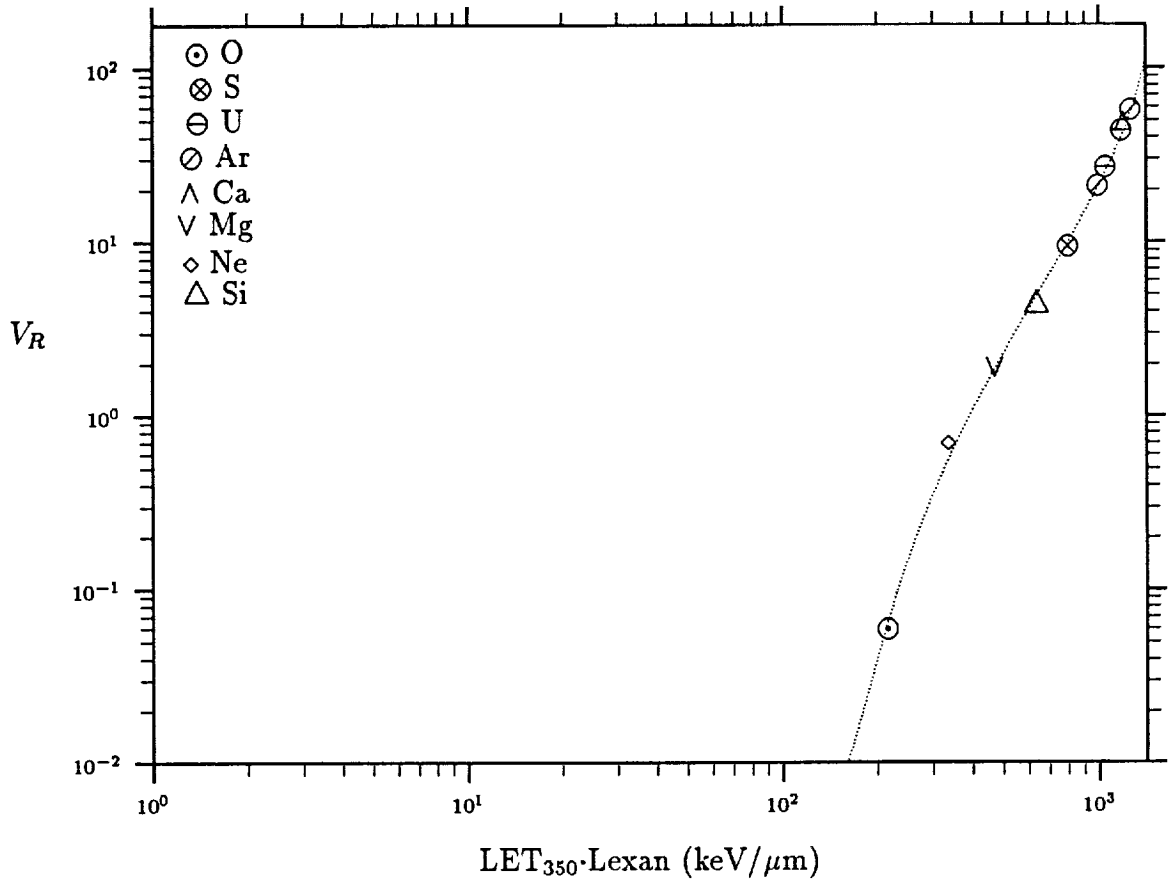

Figure 11: Polycarbonate PNTD response plot of measured V_R versus LET_{350}·Lexan for LDEF P0006 experiment.

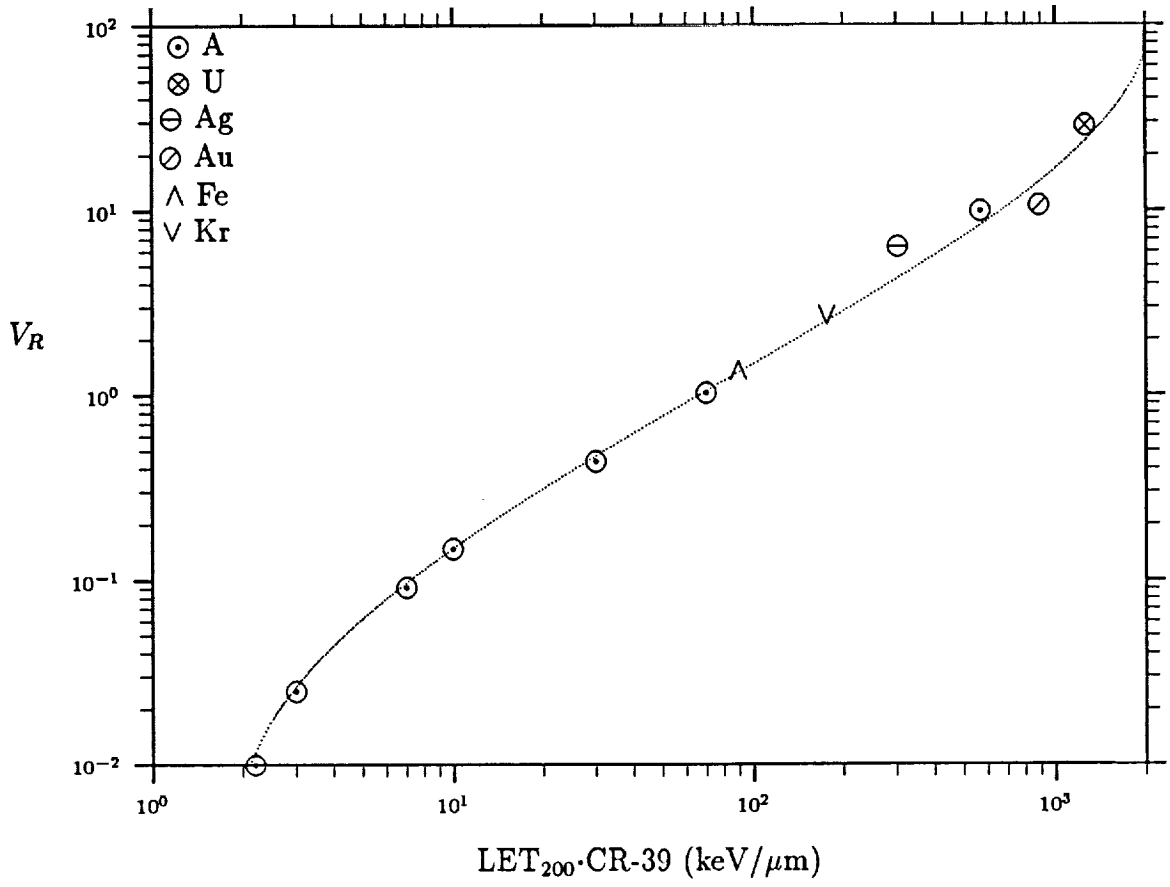

Figure 12: CR-39 PNTD response plot of measured V_R versus LET_{200}·CR-39 for LDEF P0006 experiment. Points labeled "A" are from 168 hour etch for this material adjusted to etch conditions of the P0006 CR-39 detectors.

Processing and Preliminary Analysis of P0006 PNTDs

Following the establishment of chemical processing times and the determination of detector response equations, several layers of Sheffield polycarbonate and of pure and doped CR-39 were removed from the P0006 experiment stack for preliminary analysis. Sheffield polycarbonate detectors 145G-1 and 146G-1 were etched for a period of 144 hours in 6.25 N NaOH at 50°C. CR-39 detectors 7-119 and 7-120 and CR-39 detectors with DOP additive 119BD and 120BD were etched for 36 hours in 6.25 N NaOH at 50°C.

These detectors were chosen from Stack #3 in the center of the P0006 experiment module. Those detectors chosen for processing of a given type of material were adjacent to one another in the P0006 stack. After chemical processing, the adjacent layers of detector were reassembled into their flight configuration relative to one another. The two reassembled layers are called a doublet and are analyzed as a single unit. Figure 13 illustrates a cross sectional view of a doublet.

The CR-39 doublets were scanned for coincident pairs of tracks. The doublet is placed on the stage of a optical microscope and the operator focuses on the bottom surface of the upper layer (surface 2 in Figure 13). He then scans for nuclear tracks. In the case of P0006, the detectors were nearly saturated with tracks. When a track on this second surface is found, the operator focuses onto the third surface, the upper surface of the bottom CR-39 layer, and tries to locate the companion track. The companion track is one made by the same particle. Hence the companion track has the same angle relative to the inner surface of the detector and has a polar angle (angle of the track on the $x-y$ plane of the detector) 180° removed from the second surface track. Together the two tracks represent a coincident pair. The operator then scans the first and fourth surfaces (top surface of the top layer and bottom surface of the bottom layer) for the additional possible two tracks made by the passage of the particle through the bulk of the detector.

The coincident pair method of analysis allows tracks to be categorized. Tracks in a single surface are tracks made either by very short range secondaries or by particles passing through the detector material before the stacks were assembled and hence before the period of the experiment. Tracks on the two inner surfaces of the detector are usually the result of trapped protons and are called short range (SR) tracks. Particles which leave tracks on all four surfaces of the doublet are usually galactic cosmic rays (GCR). The coincident pair method permits the exclusion of tracks made before the period of the experiment and allows the remaining particle events to be divided into two categories, two surface and four surface events, which roughly correspond to the trapped proton and galactic cosmic ray components of the low earth orbit radiation environment.

When the coincident pair tracks are located, the parameters of the second surface tracks are measured and the LET of the particle is calculated using the detector response equation. The integral LET spectra for flux, dose rate and dose equivalent rate are then generated.

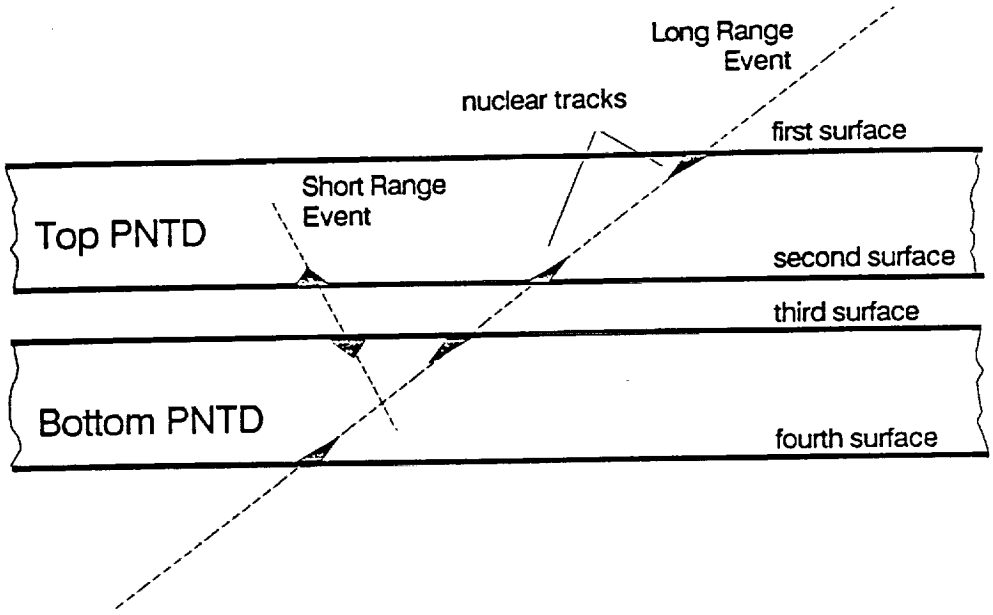

Figure 13: Cross sectional view of PNTD doublet.

Table 13: Etch parameters and fluences of P0006 PNTDs.

Sample / Material	Etch Period (hours)	Bulk Etch (μm)	GCR Fluence (events/cm^2)	SR Fluence (events/cm^2)	Total Fluence (events/cm^2)
7-119/120 CR-39	36	8.574	9.44×10^2	2.077×10^4	2.172×10^4
119/120 DOP CR-39	36	8.668	1.5×10^3	2.067×10^4	2.217×10^4
145/146G Sheffield	144	35.133	N/A	N/A	8.694×10^3

Table 14: Flux, Dose Rate and Dose Equivalent Rate for $LET_\infty \cdot H_2O \geq 5$ keV/μm measured from 7-119/120 pure CR-39 doublet.

	Flux ($cm^{-2}s^{-1}sr^{-1}$)	Dose Rate (mrad/d)	Dose Equiv. Rate (mrem/d)
Total	1.214×10^{-4}	7.793×10^{-1}	9.069×10^0
GCR	8.213×10^{-6}	1.329×10^{-1}	2.045×10^0
SR	1.132×10^{-4}	6.463×10^{-1}	7.024×10^0

LET spectra were generated for both types of CR-39 detector (with and without DOP). Due to the very low fluence of four surface tracks on the Sheffield polycarbonate, no LET spectra were derived from measurements of this material to date.

Discussion of Preliminary PNTD Results

Table 13 lists the etch duration, bulk etch and fluence for the three sets of PNTD doublets analyzed to date. LET spectra have been generated for both the CR-39 and the CR-39/DOP doublets. No LET spectra was generated for the Sheffield polycarbonate doublet due to the small number of four surface events found. The fluence given for the Sheffield polycarbonate is for single surface tracks. These are mostly stopping secondaries from collisions between incident particles and the nuclei of the stopping material.

Figures 14, 15 and 16 are the integral LET flux, dose rate and dose equivalent rate spectra measured from the pure CR-39. Tables 14 and 15 list the flux, dose and dose equivalent rates for particles with $LET_\infty \cdot H_2O \geq 5$ keV/μm and $LET_\infty \cdot H_2O \geq 100$ keV/μm respectively measured on the pure CR-39 detectors. Figures 17, 18 and 19 are the integral LET flux, dose rate and dose equivalent rate spectra measured from CR-39 with DOP. Tables 16 and 17 list the flux, dose and dose equivalent rates for particle with $LET_\infty \cdot H_2O \geq 5$ keV/μm and $LET_\infty \cdot H_2O \geq 100$ keV/μm respectively measured on the CR-39 detectors with DOP.

There is good agreement between the pure and doped CR-39 detectors. In most cases,

Table 15: Flux, Dose Rate and Dose Equivalent Rate for LET_{∞}·H_2O $\geq$100 keV/μm measured from 7-119/120 pure CR-39 doublet

	Flux ($cm^{-2}s^{-1}sr^{-1}$)	Dose Rate (mrad/d)	Dose Equiv. Rate (mrem/d)
Total	9.809×10^{-6}	2.605×10^{-1}	4.692×10^{0}
GCR	3.508×10^{-6}	8.374×10^{-2}	1.470×10^{0}
SR	6.300×10^{-6}	1.768×10^{-1}	3.222×10^{0}

Table 16: Flux, Dose Rate and Dose Equivalent Rate for LET_{∞}·H_2O $\geq$5 keV/μm measured from BD119/120 CR-39 with DOP.

	Flux ($cm^{-2}s^{-1}sr^{-1}$)	Dose Rate (mrad/d)	Dose Equiv. Rate (mrem/d)
Total	1.189×10^{-4}	8.018×10^{-1}	9.062×10^{0}
GCR	5.171×10^{-6}	7.954×10^{-2}	1.187×10^{0}
SR	1.137×10^{-4}	7.223×10^{-1}	7.874×10^{0}

Table 17: Flux, Dose Rate and Dose Equivalent Rate for LET_{∞}·H_2O $\geq$100 keV/μm measured from BD119/120 CR-39 with DOP.

	Flux ($cm^{-2}s^{-1}sr^{-1}$)	Dose Rate (mrad/d)	Dose Equiv. Rate (mrem/d)
Total	9.250×10^{-6}	2.403×10^{-1}	4.321×10^{0}
GCR	1.985×10^{-6}	4.817×10^{-2}	8.493×10^{-1}
SR	7.265×10^{-6}	1.921×10^{-1}	3.471×10^{0}

Table 18: Shielding (minimum) for P0006 Layers 119 and 120.

From top of stack:

- 2.20 g/cm^{2}Al;
- 5.67 g/cm^{2}Plastic and Fiberglass;
- 7.90 g/cm^{2}Total.

From side of stack*:

CR-39 without DOP:

- 0.64 g/cm^{2}Al;
- 0$\longrightarrow$5.8 g/cm^{2}Plastic.

CR-39 with DOP:

- 0.64 g/cm^{2}Al;
- 4.8$\longrightarrow$7.0 g/cm^{2}Plastic.

*Includes only canister and stack.

flux, dose rate, and dose equivalent rates differ only in the second significant figure. These differences are probably due to differences in shielding. Table 18 gives the shielding for the two CR-39 doublets. The CR-39/DOP doublet was contained in the center of the stack, surrounded by a cut out of other material while the pure CR-39 doublet extended from the CR-39/DOP to the edges of the stack. Thus the CR-39/DOP doublet had somewhat greater and more uniform shielding than the pure CR-39 doublet.

For chemical processing of short duration, the surfaces of the CR-39 PNTDs and the polycarbonate PNTDs were visually clear. High fluences ($\sim$ 10^4 tracks/cm^2) of primary and secondary particle tracks were seen in CR-39 and fairly high fluences ($\sim$ 10^3 tracks/cm^2) of secondary particle tracks were seen in both Tuffak and Sheffield polycarbonate. Preliminary processing of Melinex polyester PNTD will be carried out next. Selected layers of CR-39, CR-39 with DOP, Sheffield and Tuffak will now be processed and analyzed for determination of LET spectra at different shielding depths.

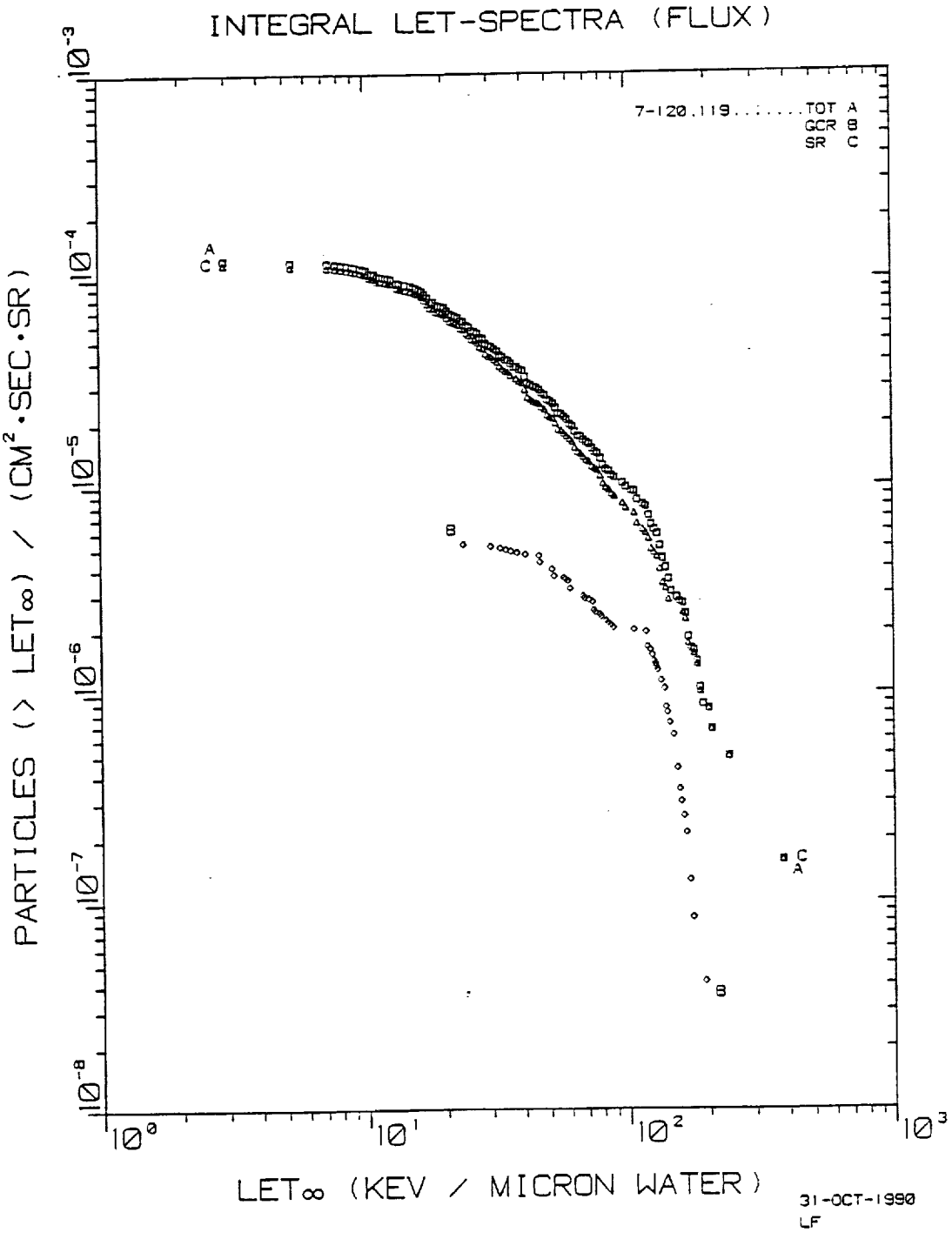

Figure 14: LET Flux spectra for 7-119/120 CR-39 without DOP. Note the separation of data into Short Range (SR) and Galactic Cosmic Ray (GCR) components.

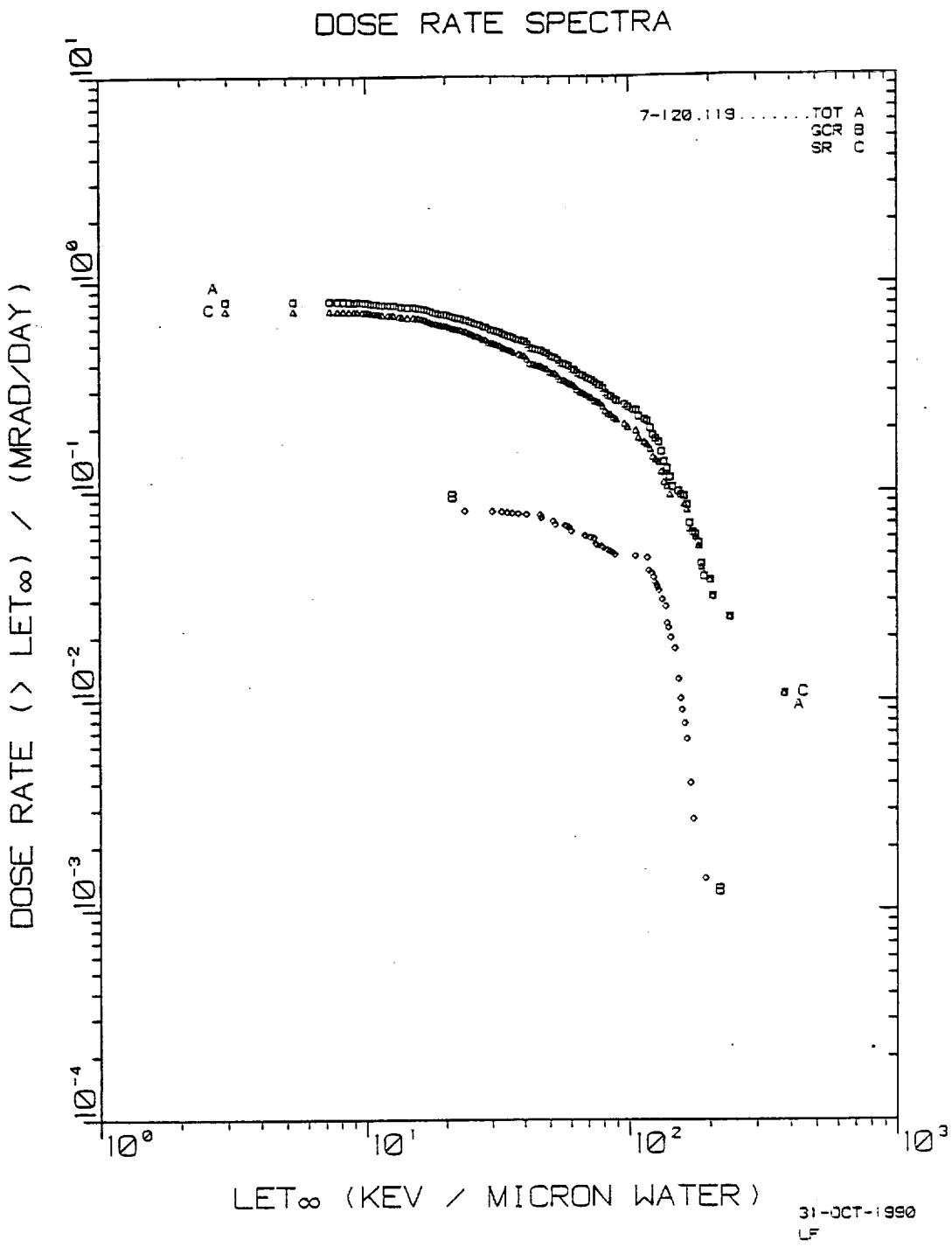

Figure 15: LET Dose Rate spectra for 7-119/120 CR-39 without DOP.

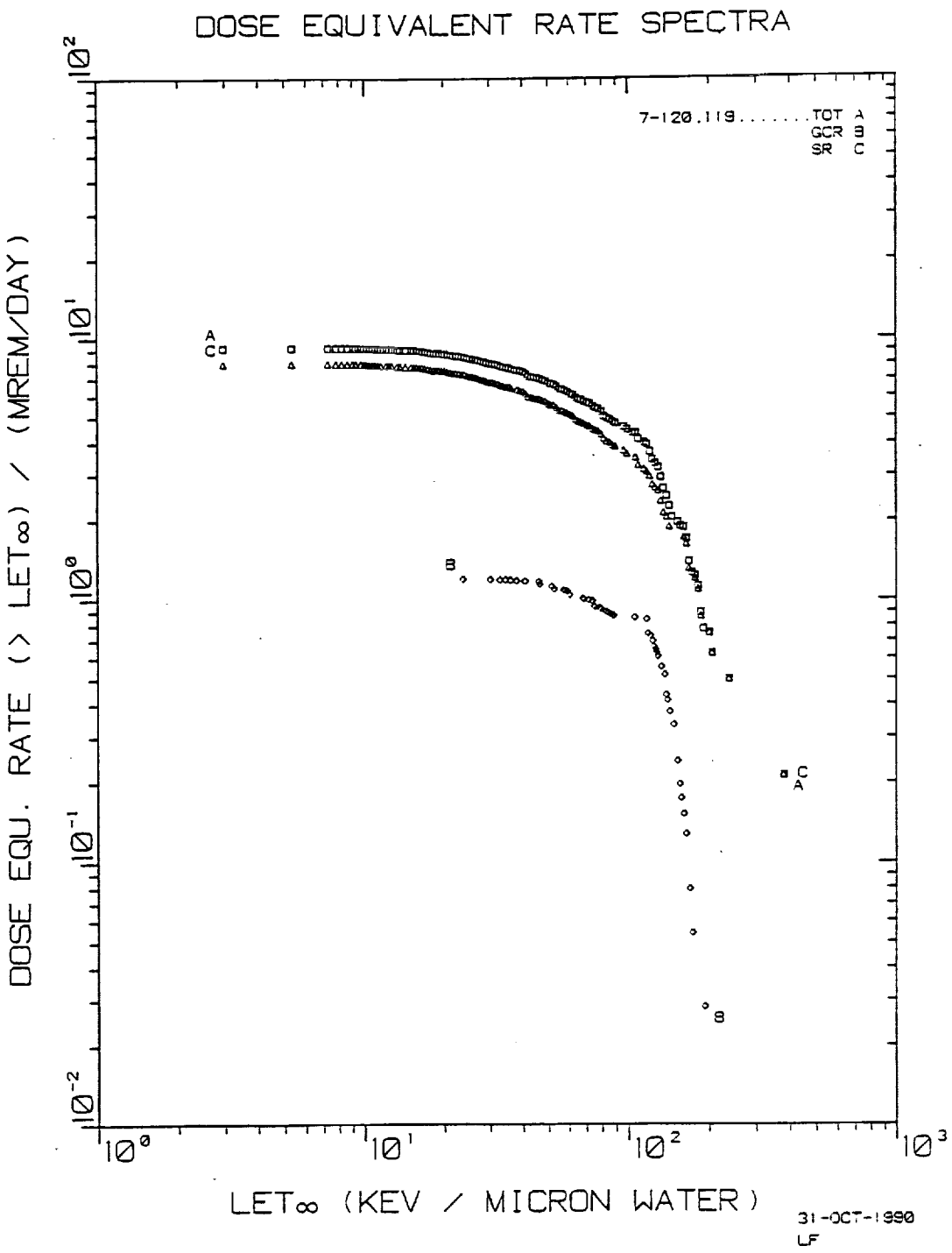

Figure 16: LET Dose Equivalent Rate spectra for 7-119/120 CR-39 without DOP.

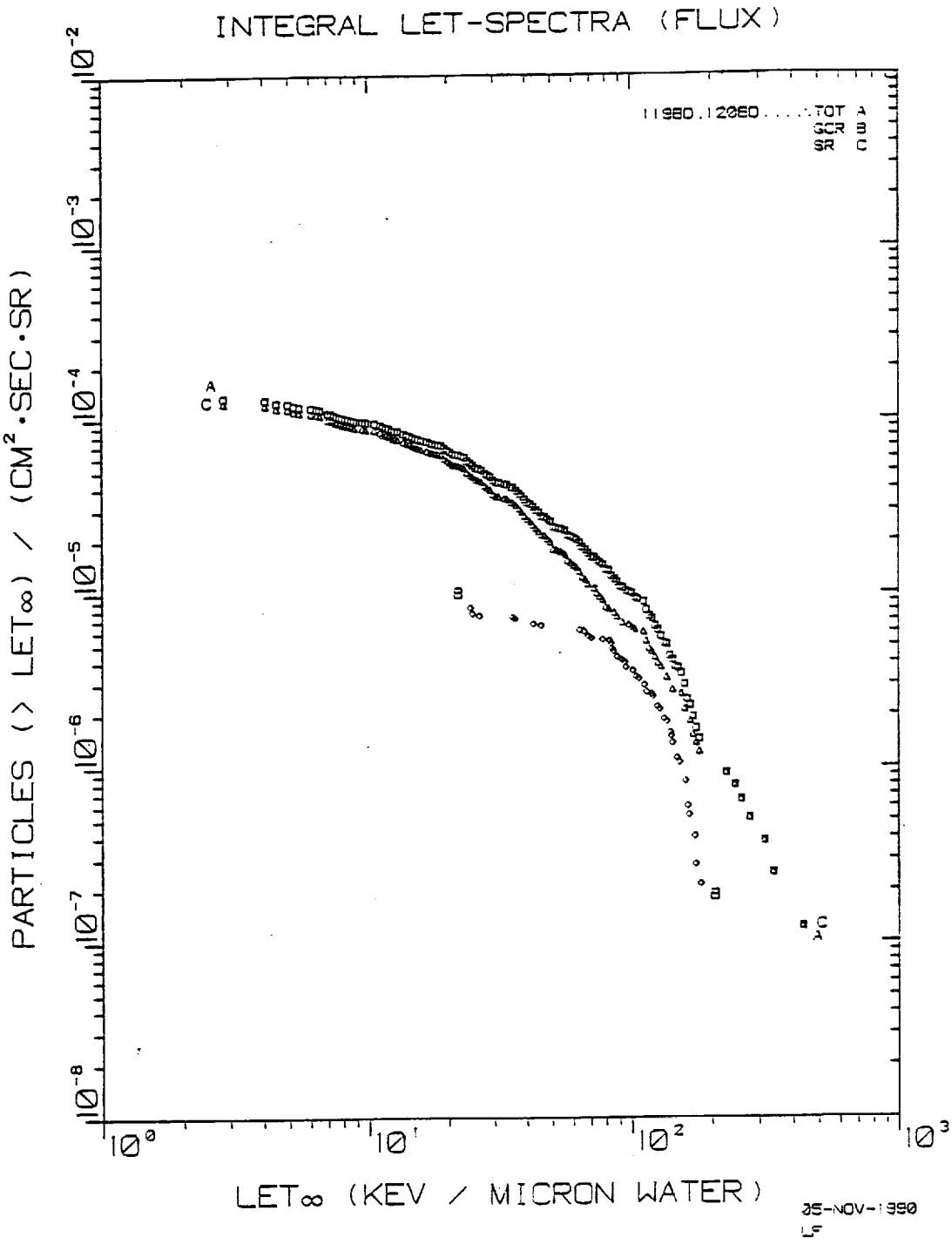

Figure 17: LET Flux spectra for BD119/120 CR-39 with DOP.

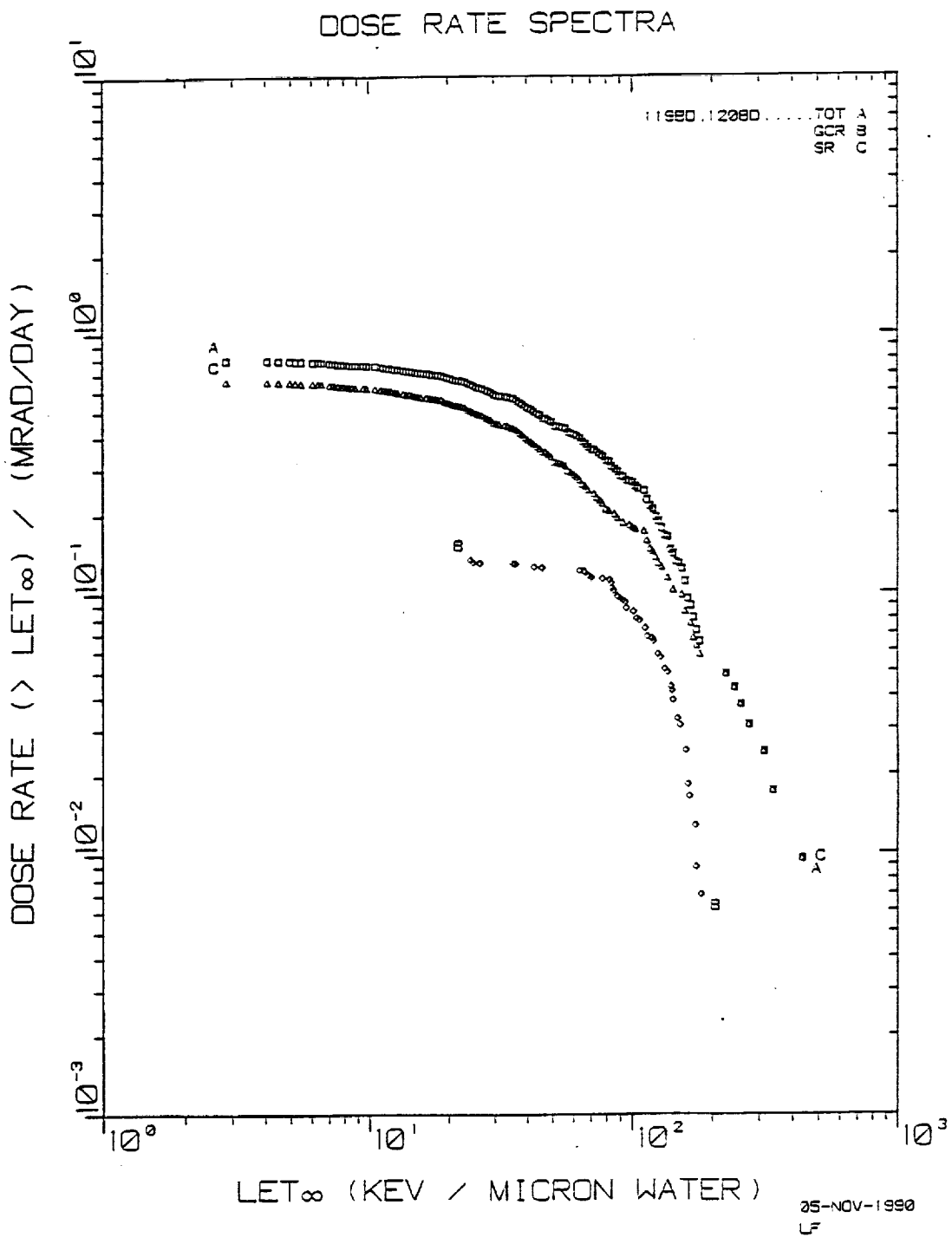

Figure 18: LET Dose Rate spectra for BD119/120 CR-39 with DOP.

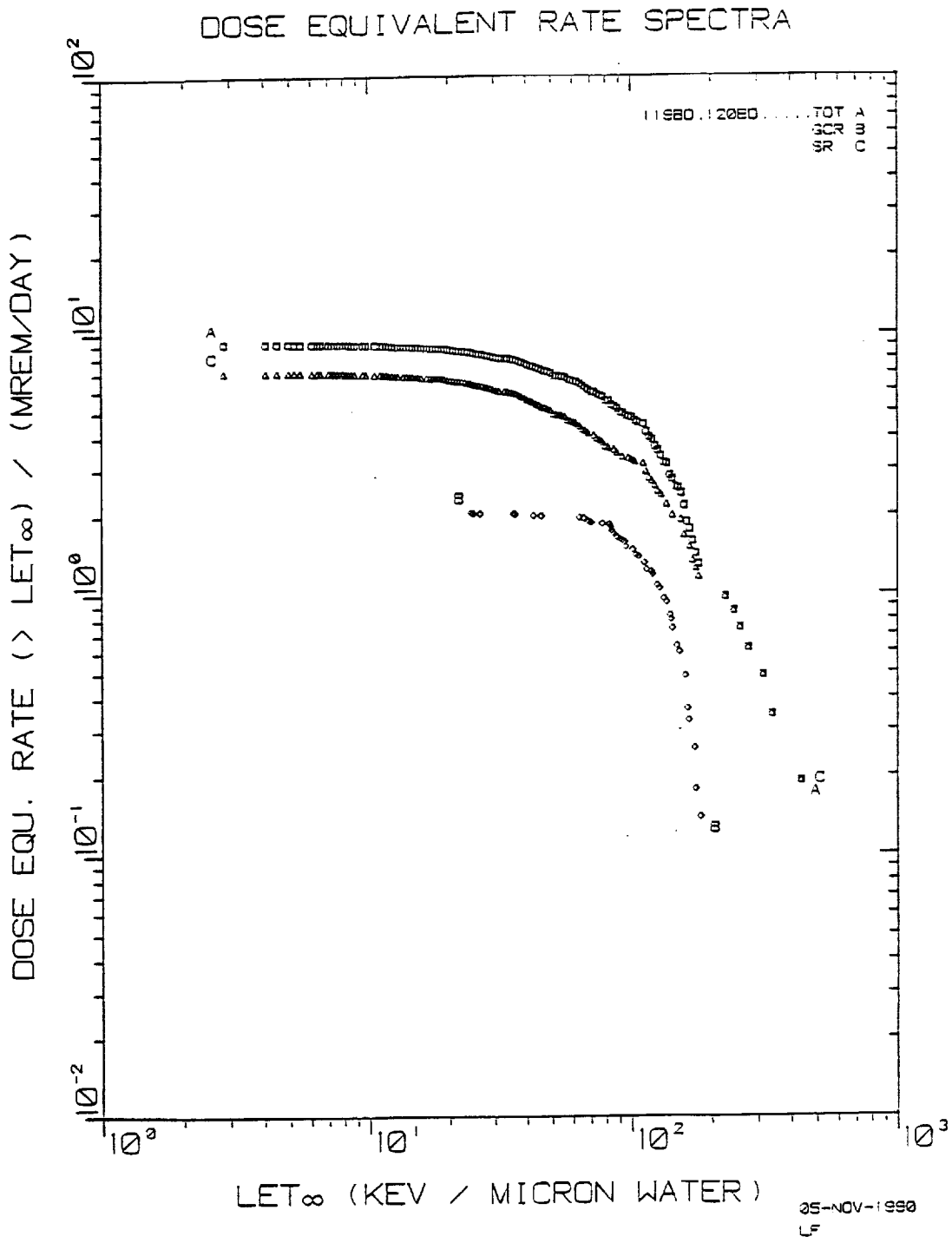

Figure 19: LET Dose Equivalent Rate spectra for BD119/120 CR-39 with DOP.

References

[1] Armstrong, T.W., and Colborn, B.L., "Scoping Estimates of the LDEF Satellite Induced Radioactivity", SAIC-90/1462, 1990.

[2] Benton, E.V., Henke, R.P., Frank, A.L., Johnson, C.S., Cassou, R.M., Tran, M.T., and Etter, E., (1981) "Space Radiation Dosimetry Aboard Cosmos 1129: U.S. Portion of Experiment K-309", in *Final Reports of U.S. Plant and Radiation Experiments Flown on the Soviet Satellite Cosmos 1129*, NASA T.M. 81288, Ames Research Center, M.R. Heinrich and K.A. Souza (editors).

[3] Berrios, W.M., (1990) "Long Duration Exposure Facility: Post-Flight Thermal Analysis, Orbital/Thermal Environment Data Package", NASA/LaRC.

[4] Dobson, P.N., Jr., and Midkiff, A.A., (1970) "Explanation of Supralinearity in Thermoluminesence of LiF in Terms on an Interacting Track Model", *Hlth. Phys.*, **18**, 571-573.

[5] Frank, A.L., Yang, D., Atallah, T., and Benton, E.V., (1990) "Review of Radiation Measurements on Selected STS Missions and Environmental Effects in PNTDs", USF-TR-78.

[6] Lomanov, M.F., Shimchuk, G.G., and Yakovlev, R.M., (1979) "Solid State Detectors of Fission Fragments for the REM-Dose Measurement of Mixed Proton and Neutron Radiation", *Hlth. Phys.*, **37**, 677-686.

[7] Stehn, J.R., Goldberg, M.D., Wiener-Chasmon, R., Mughabghab, S.F., Magurno, B.A., and May, V.M., (1965) "Neutron Cross Sections, Vol. III", BNL 325.

[8] Wollenberg, H.A., and Smith, A.R., (1969) "Energy and Flux Determinations of High-Energy Nucleons", UCRL-19364.